Paradoxical Role of Large-Conductance Calcium-Activated K$^+$ (BK) Channels in Controlling Action Potential-Driven Ca^{2+} Entry in Anterior Pituitary Cells

Fredrick Van Goor,[1] Yue-Xian Li,[2] and Stanko S. Stojilkovic[1]

[1]*Endocrinology and Reproduction Research Branch, National Institute of Child Health and Human Development, National Institutes of Health, Bethesda, Maryland 20892-4510, and* [2]*Departments of Mathematics and Zoology, University of British Colombia, Vancouver, British Columbia, Canada V6T 1Z2*

Activation of high-conductance Ca^{2+}-activated K$^+$ (BK) channels normally limits action potential duration and the associated voltage-gated Ca^{2+} entry by facilitating membrane repolarization. Here we report that BK channel activation in rat pituitary somatotrophs prolongs membrane depolarization, leading to the generation of plateau-bursting activity and facilitated Ca^{2+} entry. Such a paradoxical role of BK channels is determined by their rapid activation by domain Ca^{2+}, which truncates the action potential amplitude and thereby limits the participation of delayed rectifying K$^+$ channels during membrane repolarization. Conversely, pituitary gonadotrophs express relatively few BK channels and fire single spikes with a low capacity to promote Ca^{2+} entry, whereas an elevation in BK current expression in a gonadotroph model system leads to the generation of plateau-bursting activity and high-amplitude Ca^{2+} transients.

Key words: somatotrophs; gonadotrophs; bursting; voltage-gated Ca^{2+} channels; delayed rectifier K$^+$ channels; domain Ca^{2+}

Although all secretory anterior pituitary cells are of the same origin, they differ with respect to their Ca^{2+} signaling and secretory patterns (Stojilkovic and Catt, 1992; Kwiecien and Hammond, 1998). A majority of somatotrophs *in vitro* generate spontaneous high-amplitude fluctuations in intracellular Ca^{2+} concentration ($[Ca^{2+}]_i$) that are abolished by the removal of extracellular Ca^{2+} or by the addition of Ca^{2+} channel agonists and antagonists (Lewis et al., 1988; Tomic et al., 1999). In parallel to Ca^{2+} signaling, growth hormone secretion from anterior pituitary cells in perifusion or static incubation experiments is high in the absence of any stimuli, and this basal secretion is inhibited by extracellular Ca^{2+} removal (Stojilkovic et al., 1988; Tomic et al., 1999). Gonadotrophs also exhibit extracellular Ca^{2+}-dependent and dihydropyridine-sensitive $[Ca^{2+}]_i$ fluctuations; however, these $[Ca^{2+}]_i$ fluctuations are much smaller in amplitude than those observed in somatotrophs (Stojilkovic et al., 1992; Li et al., 1995; Kwiecien and Hammond, 1998). Moreover, basal-luteinizing hormone release is low and is not affected by the removal of extracellular Ca^{2+} or the inhibition of voltage-gated Ca^{2+} channels (VGCC; Stojilkovic et al., 1988). Such a difference in the Ca^{2+} signaling and secretory patterns between somatotrophs and gonadotrophs is in accord with their modes of regulation by hypothalamic neurohormones. Growth hormone secretion is stimulated by growth hormone-releasing hormone (GHRH) and other known releasing factors and is inhibited by somatostatin and dopamine (Muller et al., 1999). In contrast, luteinizing hormone release is stimulated by gonadotropin-releasing hormone, whereas no known hypothalamic inhibitory factors have been identified (Sealfon et al., 1997).

The ionic and cellular mechanisms that endow somatotrophs, but not gonadotrophs, with the ability to generate high-amplitude $[Ca^{2+}]_i$ transients that are sufficient to trigger exocytosis in the absence of hypothalamic or local control are not known. Here we examined the patterns of action potential (AP) firing and the underlying $[Ca^{2+}]_i$ signals in female rat somatotrophs and gonadotrophs by simultaneous measurements of membrane potential and $[Ca^{2+}]_i$ in perforated patch-clamped cells. Our results revealed that, although a majority of somatotrophs and gonadotrophs exhibit spontaneous AP firing, there are distinct differences in the profile of the AP waveform and its capacity to drive Ca^{2+} entry between the two cell types. In somatotrophs, plateau-bursting activity accounts for the generation of the high-amplitude $[Ca^{2+}]_i$ transients, whereas single spiking accounts for the low-amplitude $[Ca^{2+}]_i$ transients in gonadotrophs. In an extensive search for the underlying ionic currents mediating the discrete patterns of AP-driven Ca^{2+} entry and secretion in these two anterior pituitary cell types, our experiments revealed selective expression of the large-conductance calcium-activated K$^+$ (BK) channels in somatotrophs. Furthermore, in contrast to the typical negative feedback role of BK channels in controlling voltage-gated Ca^{2+} influx observed in other cell types (Kaczorowski et al., 1996; Sah, 1996; Vergara et al., 1998), these channels in somatotrophs act as positive feedback regulators of AP-driven Ca^{2+} entry by promoting the generation of the plateau bursting. Finally, we addressed the mechanism for such a paradoxical role of BK channels in controlling AP-driven Ca^{2+} entry in somatotrophs.

MATERIALS AND METHODS

Pituitary cell culture and cell identification. Anterior pituitary glands were excised from adult female Sprague Dawley rats (Taconic Farms, Ger-

mantown, NY) and dispersed into single cells by using a trypsin/DNase (Sigma, St. Louis, MO) cell dispersion procedure as described previously (Stojilkovic et al., 1988). Enriched somatotroph populations were obtained via a discontinuous Percoll density-gradient cell separation procedure as described previously (Koshimizu et al., 2000). Somatotrophs were identified further by their cell type-specific morphology and responses to the known neuroendocrine modulators GHRH and somatostatin. Gonadotrophs were identified initially by their cell type-specific morphology and, subsequent to experimentation, by the addition of gonadotropin-releasing hormone, which stimulates small-conductance Ca^{2+}-activated (SK) K^+ current and $[Ca^{2+}]_i$ oscillations only in gonadotrophs (Stojilkovic et al., 1992; Tse and Hille, 1992).

Electrophysiology. Current- and voltage-clamp recordings were performed at room temperature with an Axopatch 200B patch-clamp amplifier (Axon Instruments, Foster City, CA) and were low-pass filtered at 2 kHz. Unless otherwise indicated, all ionic currents and membrane potentials were measured with the perforated patch recording technique (Rae et al., 1991). Briefly, an amphotericin B (Sigma) stock solution (60 mg/ml) was prepared in DMSO and stored for up to 1 week at $-20°C$. Just before use the stock solution was diluted in pipette solution and sonicated for 30 sec to yield a final amphotericin B concentration of 240 $\mu g/ml$. Patch electrodes used for perforated patch recordings were fabricated from borosilicate glass (1.5 mm outer diameter; World Precision Instruments, Sarasota, FL) with a Flaming Brown horizontal puller (P-87, Sutter Instruments, Novato, CA). Electrodes were heat-polished to a final tip resistance of 3–6 MΩ and then coated with Sylgard (Dow Corning, Midland, MI) to reduce pipette capacitance. Pipette tips were immersed briefly in amphotericin B-free solution and then backfilled with the amphotericin B-containing solution. A series resistance of <15 MΩ was reached 10 min after the formation of a gigaohm seal (seal resistance, >5 GΩ) and remained stable for up to 1 hr. When necessary, series resistance compensation was optimized. All current recordings were corrected for linear leakage and capacitance by using a P/-N procedure. An average membrane capacitance (C_m) of 4.6 ± 0.2 and 7.5 ± 0.2 pF was recorded in somatotrophs and gonadotrophs, respectively. Pulse generation, data acquisition, and analysis were done with a PC equipped with a Digidata 1200 analog-to-digital (A/D) interface in conjunction with Clampex 8 (Axon Instruments). All values in the text are reported as mean ± SEM. Differences between groups were considered to be significant when $p < 0.05$, using the paired Student's t test.

Simultaneous recording of $[Ca^{2+}]_i$ and membrane potential or current. Pituitary cells were incubated for 15 min at 37°C in phenol red-free medium 199 containing Hanks' salts, 20 mM sodium bicarbonate, 20 mM HEPES, and 0.5 μM indo-1 AM (Molecular Probes, Eugene, OR). Membrane potential or ionic current was recorded as described above, and bulk $[Ca^{2+}]_i$ was monitored simultaneously by a Nikon photon counter system as described previously (Van Goor et al., 2000). The membrane potential or current and bulk $[Ca^{2+}]_i$ were captured simultaneously at the rate of 5 kHz, using a PC that was equipped with a Digidata 1200 A/D interface in conjunction with Clampex 8 (Axon Instruments). The $[Ca^{2+}]_i$ was calibrated *in vivo* according to Kao (1994), and the values for R_{min}, R_{max}, $S_{f,480}/S_{b,480}$, and K_D were determined to be 0.75, 3.40, 2.45, and 230 nM, respectively. In some cases the net change in $[Ca^{2+}]_i$ was reported and was determined by subtracting the baseline $[Ca^{2+}]_i$ from the peak $[Ca^{2+}]_i$ that was reached during the spike waveform or command potential.

Chemicals and solutions. For the recording of electrical membrane activity and total ionic current, the extracellular medium contained (in mM): 120 NaCl, 2 CaCl₂, 2 MgCl₂, 4.7 KCl, 0.7 MgSO₄, 10 glucose, and 10 HEPES, pH-adjusted to 7.4 with NaOH, and the pipette solution contained (in mM): 50 KCl, 90 K^+-aspartate, 1 MgCl₂, and 10 HEPES, pH-adjusted to 7.2 with KOH. So that the delayed rectifying K^+ current (I_{DR}) could be isolated, the bath contained paxilline, apamin [to block the large- and small-conductance (SK) calcium-activated K^+ currents ($I_{K_{Ca}}$)], and tetrodotoxin (to block voltage-gated Na^+ currents). To isolate voltage-dependent Ca^{2+} currents (I_{Ca}) or to introduce exogenous Ca^{2+} buffers into the cytosol, we used conventional whole-cell recording techniques. For isolated calcium current recordings, 20 mM TEA and 0.001 mM tetrodotoxin were added to the extracellular medium, and the pipette contained (in mM): 120 CsCl, 20 TEA-Cl, 4 MgCl₂, 10 EGTA, 9 glucose, 20 HEPES, 0.3 Tris-GTP, 4 Mg-ATP, 14 CrPO₄, and 50 U/ml creatine phosphokinase, pH-adjusted to 7.2 with Tris base. For the introduction of exogenous Ca^{2+} buffers into the cytoplasm, 20 mM NaCl and 100 nM apamin were added to the extracellular medium, and the pipette contained (in mM): 130 K^+-aspartate, 10 KCl, 1 MgCl₂, 9

glucose, 20 HEPES, 0.3 Tris-GTP, 4 Mg-ATP, 14 CrPO₄, 50 U/ml creatine phosphokinase, and 0.1 EGTA or 0.1 BAPTA, pH-adjusted to 7.2 with KOH. Under these whole-cell recording conditions there was no "rundown" in I_{Ca} (data not shown). All reported membrane potentials and ionic currents were corrected on-line for a liquid junction potential of +10 mV between the pipette and bath solution, except for I_{Ca}, which required no correction (Barry, 1994). The bath contained <500 μl of saline and was perifused continuously at a rate of 2 ml/min via a gravity-driven superfusion system. Stock solutions of iberiotoxin and apamin were prepared in double-distilled deionized water, whereas stock solutions of paxilline and BAPTA AM were prepared in DMSO. All chemicals were obtained from Sigma and Aldrich (Milwaukee, WI).

Gonadotroph model cell. To simulate the expression of BK channels and their impact on the pattern of AP firing in pituitary cells, we used the previously developed mechanistic biophysical model of gonadotrophs (Li et al., 1995). This gonadotroph model cell was based on experimentally derived electrical membrane and ionic channel properties and included the following conductances: a leak current, two types of Ca^{2+} channels (an L-type and a T-type), and two types of K^+ channels (the delayed rectifier and the SK-type Ca^{2+}-activated K^+ channel). Because SK K^+ channels are activated by Ca^{2+} inside the cell, Ca^{2+} handling in these cells was modeled by taking into account Ca^{2+} entry through VGCC, Ca^{2+} extrusion by plasma membrane Ca^{2+} pumps, and Ca^{2+} release and uptake by a passive intracellular Ca^{2+} store. The original model did not include a BK channel and exhibited tonic spiking activity similar to that observed in native gonadotrophs (for details, see Li et al., 1995).

In the present study the impact of BK channel expression on the pattern of AP firing in gonadotrophs was examined by incorporating a BK-type K^+ channel into the original gonadotroph cell model. To do this, we modified the original gonadotroph cell model in two ways: (1) a BK-type Ca^{2+}-activated K^+ current (I_{BK}) was incorporated into the voltage equation, and (2) the cytosolic space was divided into two interconnected subcompartments: a submembrane shell and an interior core region. To simulate the changes in $[Ca^{2+}]_i$ occurring near the open pore of the VGCC (domain Ca^{2+}; C_d) in the gonadotroph model cell, we modeled the profile of Ca^{2+} distribution in a buffered medium near a point source of Ca^{2+} flux. The concentration profiles can be approximated by hemispherically symmetric steady-state solutions to partial differential equations that describe the binding of Ca^{2+} to buffer molecules and the diffusion of Ca^{2+} and their buffers (Neher, 1998; Smith et al., 2001). We used the simplest distribution formula obtained with an excess buffer approximation (for details, see Smith et al., 2001):

$$C(r) = C_s + \sigma e^{-r/\lambda}/(2\pi Dr).$$

Here, r is the distance from the flux source, σ is the source strength, D is the diffusion rate of Ca^{2+} in the medium, C_s is the background Ca^{2+} concentration in the submembrane shell, and:

$$\lambda = (D/(k^+[B]))^{1/2},$$

is the space constant that depends on the binding constant between Ca^{2+} and the buffer k^+, the buffer concentration $[B]$, and the Ca^{2+} diffusion rate D. We assume that the average distance between the L-type channel opening and the Ca^{2+} binding site of the BK channel is 50 nm. For $D = 250$ μm/sec, $k^+ = 500$ μM^{-1}/sec, and $[B] = 200$ μM, this distance is identical to the characteristic space constant λ. To model the domain Ca^{2+} concentration at the pore of an L-type Ca^{2+} channel, we made the source strength σ equal to the average single channel flux strength:

$$\sigma = -i_{Ca-L}/2F.$$

(F is Faraday's constant). Therefore, the domain Ca^{2+} concentration:

$$C_d = C_s - I_{Ca-L}/(4e\pi NDF\lambda),$$

where I_{Ca-L} is the L-type I_{Ca} in the whole cell and N is the number of L-type Ca^{2+} channels. In the model simulation we need only to specify the value of the lumped parameter $p = 1/(4e\pi NDF\lambda)$ such that:

$$C_d = C_s - PI_{Ca-L}.$$

Implicit in this equation is the assumption that the Ca^{2+} microdomain appears and disappears instantaneously as the L-type channels open and close.

In simulations of BK channel expression into gonadotrophs, the I_{BK} was represented in the modified gonadotroph cell model by:

$$I_{BK} = g_{k-bk} b_\infty(V, C_d)\phi_K,$$

where:

$$\phi_K = V[1 - \exp(z_K F(V - V_K)/RT)]/(1 - \exp(z_K FV/RT)),$$

is the Goldman–Hodgkin–Katz driving force for K^+ channels. The gating variable b_∞ is a function of both the membrane potential V and the domain Ca^{2+} concentration at the opening of L-type Ca^{2+} channels. Because gating is fast, we assumed that the dependence of I_{BK} on V and C_d is instantaneous. This gating variable b_∞ is modeled by the formula:

$$b_\infty(V, C_d) = 1/[1 + \exp((V_b - V)/k_b)],$$

where:

$$V_b(C_d) = 52(7 - C_d)(0.12 + C_d)/(9 + C_d)/(0.02 + C_d),$$

and:

$$k_b(C_d) = 8(6 + 3C_d)/(6 + C_d),$$

with C_d in unit μM. These equations were obtained by directly fitting these expressions with experimental data on single BK channel properties in cultured rat muscle cells (Barrett et al., 1982).

In the revised model we divide the cytosolic space into a thin submembrane shell region and a spherical interior core, between which there are no barriers. Although Ca^{2+} can diffuse freely between these two compartments, they are treated as two distinct compartments to retain the differential features of Ca^{2+} signals in these two regions. The intracellular Ca^{2+} store is modeled as a distributed, passive, and linear Ca^{2+} storage space that is capable of taking up and releasing Ca^{2+} rapidly. We also assumed that the Ca^{2+} level in the store is in constant equilibrium with the bulk $[Ca^{2+}]_i$, indicating that the store behaves like a linear Ca^{2+} buffer that absorbs a fixed fraction of total intracellular Ca^{2+} at any fixed time. This reduced the number of Ca^{2+} variables to two: the submembrane concentration (C_s) and the total intracellular concentration (C_T). Other Ca^{2+} variables such as the bulk Ca^{2+} concentration in the core (C_b), and the Ca^{2+} concentration in the endoplasmic reticulum Ca^{2+} stores (C_{er}) can be expressed as a function of C_s and C_T.

The model involves seven variables: membrane potential V, four gating variables, the submembrane Ca^{2+} concentration (C_s), and the total intracellular Ca^{2+} concentration measured by the shell volume:

$$C_T = C_s + \sigma_1 C_{er} + \sigma_2 C_b,$$

where C_{er} and C_b are the concentrations in the endoplasmic reticulum (ER) Ca^{2+} store and the core, and $\sigma_1 = V^e_{er}/V^e_{sh}$ and $\sigma_2 = V^e_{bk}/V^e_{sh}$ are the ratios between the effective volumes of the ER and the core to that of the submembrane shell. The effective volume refers to the physical volume of the compartment multiplied by the respective buffering capacity. Typically, the effective cytosolic volume is ~100 times the physical volume because only ~1 of Ca^{2+} 100 ions is free in the cytosol.

$$-C_m dV/dt = (g_{ca-l}l^2 + g_{ca-t}m^2h)\phi_{Ca}$$
$$+ (g_{k-dr}n + g_{k-sk}s_\infty + g_{k-bk}b_\infty)\phi_K + g_l(V - V_L) \quad (1)$$

$$V^e_{sh} dC_s/dt = [C_{eq}(C_T) - C_s]/\tau_c - \alpha I_{Ca} - p(C_s) \quad (2)$$

$$V^e_{sh} C_T/dt = -\alpha I_{Ca} - p(C_s) \quad (3)$$

$$dq/dt = (q_\infty - q)/\tau_q (q \text{ for } l, m, n, h), \quad (4)$$

where:

$$\phi_I = V[1 - \exp(z_i F(V - V_i)/RT)]/(1 - \exp(z_i FV/RT)),$$

where i for Ca^{2+} and K^+ is the Goldman–Hodgkin–Katz driving force for ion i. Notice that the effect of varying domain Ca^{2+} concentration on ϕ_{Ca} is ignored for simplicity. For the activation gates l, m, n,

$$q_\infty = 1/[1 + \exp((V_q - V)/k_q)],$$

whereas for the inactivation gate h,

$$h_\infty = 1/[1 + \exp((V - V_h)/k_h)].$$

The voltage-dependent time constants are: $\tau_l = \tau_{0l} \cdot \tau(V)$ and $\tau_m = \tau_{0m} \cdot \tau(V)$, with:

$$\tau(V) = \exp((V_\tau - V)/k_\tau)/[1 + 2\exp(3(V_\tau - V)/k_\tau)].$$

Then,

$$s_\infty(C_s) = C_s^4/(C_s^4 + K_s^4),$$

and $b_\infty(V, C_d)$ is given in the paragraph in which the BK channel is discussed. Also,

$$I_{ca} = I_{CaL} + I_{caT} = (g_{ca-l}l^2 + g_{ca-t}m^2h)\phi_{Ca},$$

$$A = 1/(\sigma_1 + \sigma_2(1 + k_e/L)),$$

$$\tau_c = \kappa^{-1}/(1 + A),$$

$$C_{eq}(C_T) = C_T A/(1 + A),$$

$$C_b = A(C_T - C),$$

$$C_{ER} = (1 + k_e/l)C_b,$$

$$p(C_s)s_\infty(C_s) = C_s^4/(C_s^4 + K_s^4),$$

where L is the ER membrane Ca^{2+} permeability, k_e is the linear SERCA pump rate, and $p(C_s)$ is the plasma membrane Ca^{2+} pump rate.

Parameter values used in the simulations include the following: the diameter of the cell, $d = 10 \mu m$; $V^e_{sh} = 0.026$ nl, $\sigma_1 = 1$, $\sigma_2 = 0.5$, $\alpha = 0.00518 (\mu M \cdot nl)/(pA \cdot sec)$, $F/RT = 0.0375$ mV^{-1}, $C_m = 0.00314$ nF, $v_p = 0.05 (\mu M \cdot nl)/sec$, $p = 0.1 \mu M/pA$. In mV, $V_{ca} = 125$, $V_K = -85$, $V_L = -60$, $V_1 = -20$, $V_m = -30$, $V_h = -50$, $V_n = -5.1$, $V_\tau = -60$, $k_1 = 12$, $k_m = 9$, $k_h = 4$, $k_n = 12.5$, $k_\tau = 22$. In sec, $\tau_{01} = 0.0185$, $\tau_{0m} = 0.01$, $\tau_h = 0.015$, $\tau_n = 0.0225$. In μM, $K_s = 0.68$ and $K_p = 0.15$. In nl/sec, $L = 0.031$, $\kappa = 3$, and $k_e = 5$. In nS, $g_{ca-1} = 16$, $g_{ca-t} = 5$, $g_{ca-dr} = 1$, $g_{K-sk} = 0.6$, $g_{K-bk} = 0.46$, $g_1 = 0.03$.

RESULTS

Cell type-specific patterns of AP firing in pituitary cells

The patterns of AP firing and the associated changes in bulk $[Ca^{2+}]_i$ were compared between rat gonadotrophs and somatotrophs by monitoring membrane potential and $[Ca^{2+}]_i$ simultaneously. In gonadotrophs, spontaneous AP firing was observed in 52% of the cells that were examined (Fig. 1, *left panels*). In all spontaneously active gonadotrophs ($n = 26$) the electrical membrane activity was characterized by the firing of single spikes at a frequency of 0.7 ± 0.1 Hz (mean $\pm$ SEM). The spike upstroke was rapid and reached a peak amplitude of 11.2 ± 2.1 mV. Spike repolarization was also relatively rapid, limiting its duration at one-half amplitude to 43 ± 15 msec. The interspike interval was characterized by a slow pacemaker depolarization from a baseline potential of -52 ± 1 mV and culminated in the initiation of an another spike. Removal of extracellular Ca^{2+} ($n = 3$) or the addition of L-type voltage-gated Ca^{2+} channel blockers ($n = 4$) abolished spiking in all of the gonadotrophs that were examined in the present study (data not shown) and in previous studies (Stojilkovic et al., 1992; Li et al., 1995).

In somatotrophs, spontaneous AP firing was observed in 88% ($n = 34$) of the cells that were analyzed (Fig. 1, *right panels*). Unlike gonadotrophs, the electrical membrane activity was characterized by the rhythmic firing of slow-wave plateau potentials that depolarized the membrane potential from -54 ± 2 to -24 ± 1 mV. Superimposed on the plateau potentials were multiple small-amplitude fast spikes. The first spike depolarized the membrane potential to -6.4 ± 1.7 mV, and the spikes that followed progressively decreased in amplitude during the plateau potential (the ratio of the first spike amplitude to that of the last spike was ~3:1). Together, the plateau potentials and the associated small-amplitude spikes made up a single burst of electrical activity
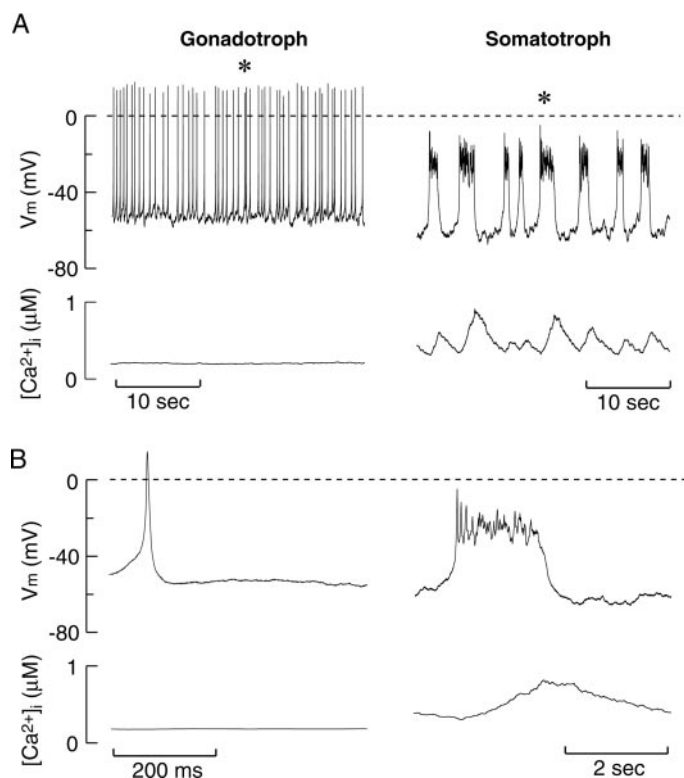
Figure 1. Distinct patterns of AP firing and $[Ca^{2+}]_i$ signaling in rat gonadotrophs and somatotrophs. *A,* Simultaneous recording of V_m and $[Ca^{2+}]_i$ in an identified gonadotroph (*left*) and somatotroph (*right*), using the perforated patch-clamp recording configuration in the current-clamp mode. *B,* Expanded time scale of the AP and associated $[Ca^{2+}]_i$ signal identified in each cell type by the *asterisks* in *A*. Representative tracings from 26 gonadotrophs and 34 somatotrophs are shown.

(hereafter referred to as plateau bursting) with a duration of 1.3 ± 0.2 sec. After each burst a pacemaker potential slowly depolarized the membrane potential toward the threshold for the next burst, resulting in a relatively slow frequency of 0.26 ± 0.03 Hz. Extracellular Ca^{2+} removal ($n = 10$) or the addition of VGCC blockers ($n = 4$) abolished plateau-bursting activity in all of the cells that were examined (data not shown).

The cell type-specific AP waveforms had different capacities to drive extracellular Ca^{2+} entry (Fig. 1). The single-spiking activity in gonadotrophs had a low capacity to drive Ca^{2+} entry, resulting in low-amplitude $[Ca^{2+}]_i$ transients (net change in $[Ca^{2+}]_i$, 30 ± 5 nM; $n = 26$). In contrast, the plateau-bursting activity in somatotrophs had a high capacity to drive extracellular Ca^{2+} entry, resulting in high-amplitude $[Ca^{2+}]_i$ transients (net change in $[Ca^{2+}]_i$, 583 ± 60 nM; $n = 34$). Despite the higher frequency of AP firing in gonadotrophs, the pattern of AP firing in somatotrophs gave rise to a higher average $[Ca^{2+}]_i$ when compared with that in gonadotrophs (average $[Ca^{2+}]_i$ measured over a 2 min period, 542 ± 54 nM in somatotrophs vs 130 ± 18 nM in gonadotrophs). These results indicate that the differences between gonadotrophs and somatotrophs with respect to the pattern of $[Ca^{2+}]_i$ signaling is attributable to the profile of the underlying AP waveforms and not to the (in)ability of each cell type to generate spontaneous AP firing.

Differential expression of BK channels between gonadotrophs and somatotrophs

We next examined whether there are differences in the ionic conductances between gonadotrophs and somatotrophs that may

account for the cell type-specific AP firing patterns and their associated $[Ca^{2+}]_i$ signals. Although a similar group of ionic channels was found in each cell type, there was a marked difference in BK channel expression between gonadotrophs and somatotrophs. This was confirmed in experiments in which the expression of BK channels was analyzed by a two-pulse protocol (Fig. 2). This protocol consisted of an initial membrane depolarization to -10 mV for 100 msec (holding potential, -90 mV) to activate VGCCs. After this Ca^{2+} influx step the membrane potential was stepped from -10 to $+90$ mV for 500 msec, during which the magnitude of peak K^+ current (I_K) activation was evaluated (Fig. 2*A*). Because $+90$ mV is near the reversal potential for Ca^{2+} under our experimental conditions, there was no net Ca^{2+} influx when the membrane potential was stepped directly to $+90$ mV from a holding potential of -90 mV (Fig. 2*B*, *bottom trace*; basal $[Ca^{2+}]_i$ vs $[Ca^{2+}]_i$ during the test pulse, 61 ± 18 vs 64 ± 19 nM; $p > 0.05$; $n = 15$). Conversely, the application of the two-pulse protocol evoked a significant and similar rise in $[Ca^{2+}]_i$ in both cells types (Fig. 2*B*, *top trace*; net change in $[Ca^{2+}]_i$: gonadotrophs, 160 ± 18 nM; somatotrophs, 155 ± 28 nM; $n = 20$). This is consistent with the similarity in the sustained voltage-gated Ca^{2+} current (I_{Ca}) density at -10 mV (somatotrophs, 4.3 ± 0.7 pA/pF; $n = 5$; gonadotrophs, 5.1 ± 0.9 pA/pF; $n = 5$) and the I_{Ca}–voltage relation in both cell types (data not shown; $n = 5$).

In gonadotrophs and somatotrophs the removal of extracellular Ca^{2+} reduced the I_K evoked during the test pulse (Fig. 2*C*), indicating the presence of a Ca^{2+}-sensitive I_K ($I_{K_{Ca}}$) in both cell types. Isolation of $I_{K_{Ca}}$ by subtracting the extracellular Ca^{2+}-dependent current from the total current indicated that its peak amplitude was much greater in somatotrophs than in gonadotrophs (Fig. 2*D*). Like extracellular Ca^{2+} removal, the application of the highly specific BK channel blockers, 1 μM paxilline (Knaus et al., 1994; Sanchez and McManus, 1996) (Fig. 2*E*) or 100 nM iberiotoxin (IBTX; Galvez et al., 1990; Giangiacomo et al., 1992) (data not shown), reduced the I_K evoked during the test pulse in both cell types. Extracellular Ca^{2+} removal in the presence of either BK channel blocker did not reduce I_K further. In addition, isolation of the BK current (I_{BK}) by subtracting the paxilline-sensitive (Fig. 2*F*) or IBTX-sensitive (Fig. 2, *legend*) current from the total current indicated that, within each cell type, the peak I_{BK} amplitude was similar to that of $I_{K_{Ca}}$. These results indicate that I_{BK} is the predominant $I_{K_{Ca}}$ activated by the two-pulse protocol in both cell types. Moreover, the magnitude of I_{BK} activation by voltage-gated Ca^{2+} entry is much greater in somatotrophs than in gonadotrophs. This is likely attributable to differences in BK channel expression, because the increase in $[Ca^{2+}]_i$ evoked by the Ca^{2+} influx step, the I_{Ca}–voltage relation, and I_{Ca} density measured at -10 mV are similar between gonadotrophs and somatotrophs (see above).

Dependence of plateau bursting on BK channel activation

The differential expression of BK channels between somatotrophs and gonadotrophs suggests that these channels may underlie the cell type-specific patterns of AP-driven $[Ca^{2+}]_i$ signaling. To test this, we examined the role of BK channels in shaping the profile of the AP waveform and the associated $[Ca^{2+}]_i$ signals in gonadotrophs and somatotrophs. We first examined whether a rise in $[Ca^{2+}]_i$ is required for I_{BK} activation and the generation of the distinct AP-firing patterns in each cell type. To do this, we examined the effects of the membrane-permeable Ca^{2+} buffer, BAPTA AM, on I_{BK} activation and the pattern of AP firing. In
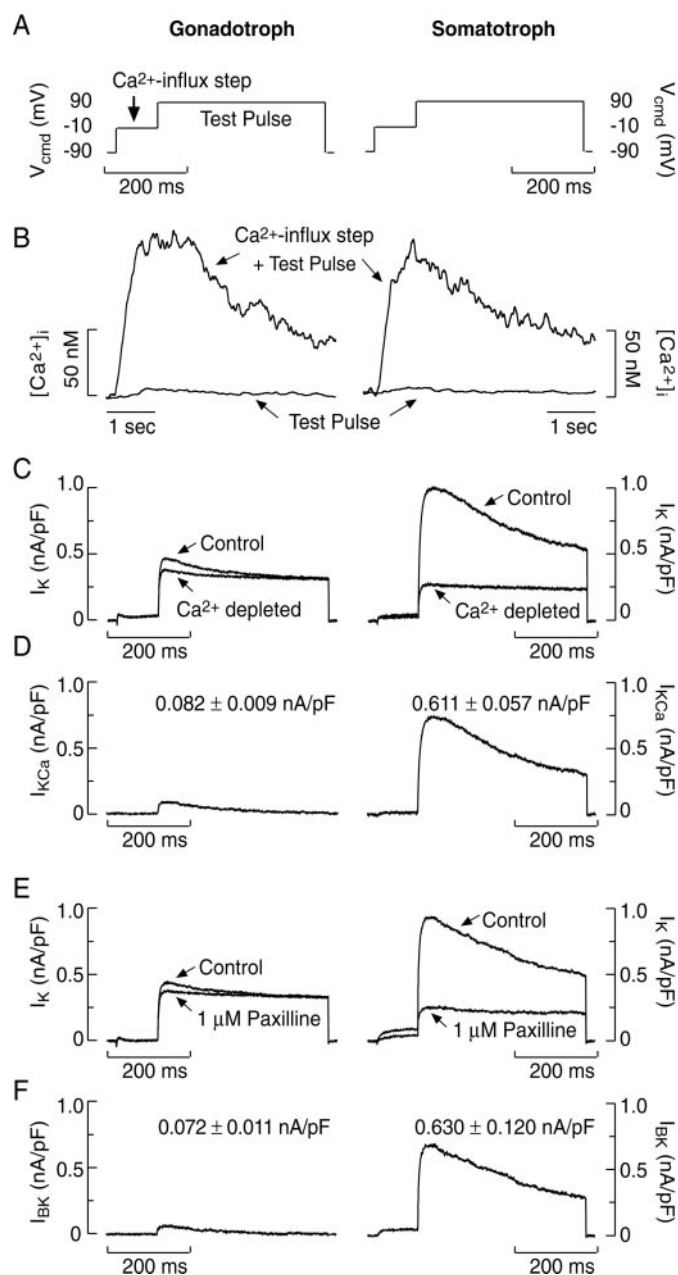
Figure 2. Differential expression of BK channels between gonadotrophs and somatotrophs. *A,* A two-pulse protocol was used to monitor $I_{K_{Ca}}$ activation by voltage-gated Ca^{2+} entry. This protocol consisted of a 100 msec conditioning pulse to -10 mV to activated VGCCs, followed by a 500 msec test pulse to $+90$ mV, during which the peak I_K was monitored. *B,* Change in $[Ca^{2+}]_i$ evoked by two-pulse protocol and by the test pulse alone in gonadotrophs (*left*) and somatotrophs (*right*). *C,* Extracellular Ca^{2+} removal reduced I_K evoked by the two-pulse protocol in gonadotrophs and somatotrophs. *D,* The net $I_{K_{Ca}}$ activated by the two-pulse protocol in gonadotrophs ($n = 9$) and somatotrophs ($n = 15$) was obtained by subtracting the current evoked in Ca^{2+}-deficient medium from the control current. *E,* Application of 1 μM paxilline reduced I_K evoked by the two-pulse protocol in gonadotrophs and somatotrophs. *F,* The net paxilline-sensitive I_{BK} activated by the two-pulse protocol in gonadotrophs ($n = 11$) and somatotrophs ($n = 15$). The mean ± SEMs of the peak $I_{K_{Ca}}$ and I_{BK} evoked during the test pulse are shown in *D* and *F,* respectively. The peak I_{BK} isolated by 100 nM IBTX subtraction in gonadotrophs ($n = 5$) and somatotrophs ($n = 10$) was 0.089 ± 0.012 and 0.521 ± 0.36 nA/pF, respectively. To account for differences in cell size between gonadotrophs and somatotrophs, we normalized all currents to the membrane capacitance of each cell that was examined.
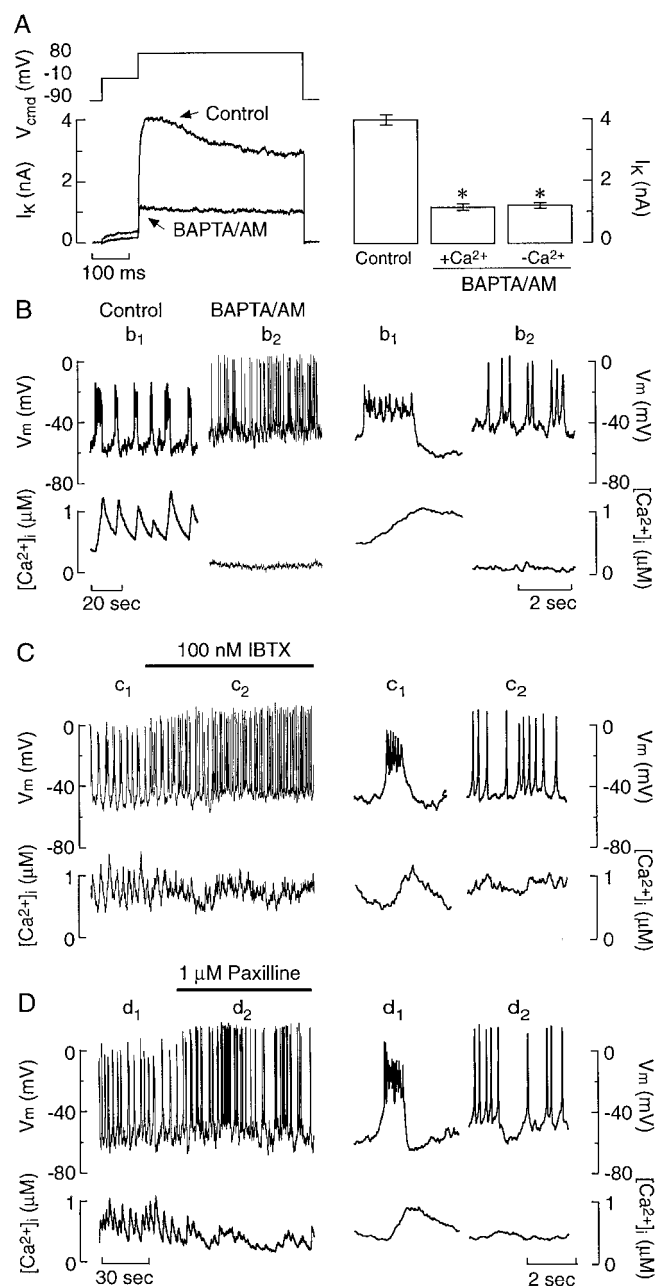
Figure 3. Dependence of the plateau-bursting activity in somatotrophs on the activation of BK channels. *A, Left,* Representative I_K tracings evoked by the two-pulse protocol in somatotrophs preincubated with DMSO (*Control*) or BAPTA AM (20 μM) for 45 min at 37°C. *A, Right,* Mean ± SEM of the peak I_K evoked by the two-pulse protocol in somatotrophs preincubated with DMSO ($n = 5$), BAPTA AM ($n = 5$), and BAPTA AM in the absence of extracellular Ca^{2+} ($n = 5$). *B, Left,* Simultaneous measurement of the membrane potential and $[Ca^{2+}]_i$ in somatotrophs preincubated with DMSO (*Control*) or BAPTA AM. *B, Right,* Expanded time scale of AP and associated $[Ca^{2+}]_i$ signals identified in the *left panel* by b_1 (*Control*) and b_2 (*BAPTA/AM*). Representative tracings from five controls and BAPTA AM-loaded somatotrophs are shown. *C, D, Left,* Simultaneous measurement of the membrane potential and $[Ca^{2+}]_i$ before and during (*horizontal bar*) the application of 100 nM IBTX ($n = 14$) or 1 μM paxilline ($n = 4$). *C, D, Right,* Expanded time scale of the AP and associated $[Ca^{2+}]_i$ signals before (c_1 and d_1) and during the application of IBTX (c_2) or paxilline (d_2).

Table 1. Effects of 100 nM IBTX and 1 μM paxilline on the profile of the AP waveform and the associated $[Ca^{2+}]_i$ transients in spontaneously active rat somatotrophs

	Control	IBTX (14)	Control	Paxilline (4)
Peak spike amplitude (mV)	-5.4 ± 1.2	$7.3 \pm 1.9^*$	-3.5 ± 1.3	$12.9 \pm 1.3^*$
Net spike repolarization (mV)	21.0 ± 1.6	$46.4 \pm 3.0^*$	26.5 ± 1.0	$58.3 \pm 2.5^*$
Net $\Delta[Ca^{2+}]_i$ (nM)	375.8 ± 97.2	$46.0 \pm 7.8^*$	438.0 ± 39.1	$123.2 \pm 27.2^*$

The net spike repolarization was measured from the peak spike amplitude to the baseline potential recorded during the interspike period. The number of trials for each drug are shown in parentheses, and the asterisks indicate a significant difference from control values ($p < 0.05$).

cells preloaded with 20 μM BAPTA AM for 45 min at 37°C, the two-pulse protocol did not activate I_{BK} in somatotrophs (Fig. 3A) or gonadotrophs (data not shown). In all five gonadotrophs that were examined, the pattern of AP firing was not affected by BAPTA AM (data not shown). In contrast, in somatotrophs preloaded with BAPTA AM, the profile of the AP waveform was shifted from plateau bursting to single spiking (Fig. 3B; $n = 5$).

Similarly, the application of 100 nM IBTX or paxilline during spontaneous AP firing in somatotrophs shifted the profile of the AP waveform from plateau bursting to single spiking, which resulted in a dramatic decrease in the amplitude of the $[Ca^{2+}]_i$ transients (Fig. 3C,D). Specifically, the peak spike amplitude was increased, and there was a marked increase in the magnitude of spike repolarization (Table 1). Consequently, the plateau-bursting potential was abolished, and the capacity of AP firing to drive Ca^{2+} entry was reduced (Table 1). In addition to the shift from phasic to tonic spiking, the application of the BK channel blockers depolarized the baseline potential from -54 ± 2 to -49 ± 2 mV ($p < 0.05$; $n = 18$) (Fig. 3). In gonadotrophs the application of 100 nM IBTX during spontaneous AP firing did not alter the amplitude (peak spike amplitude: control, 9.5 ± 3.2 mV vs IBTX, 10.4 ± 4.3 mV; $p > 0.05$; $n = 4$) or duration (spike duration at one-half amplitude: control, 10.5 ± 2.0 msec vs IBTX, 12.7 ± 2.8 msec; $p > 0.05$; $n = 4$) of the single spikes. These results indicate that BK channel activation is required for generating the sustained plateau potential in somatotrophs, which prolongs AP duration and facilitates extracellular Ca^{2+} entry.

BK channels limit delayed rectifying K$^+$ channel activation

We next examined the ionic mechanisms underlying the apparent paradoxical role of BK channels in facilitating AP-driven Ca^{2+} entry in rat somatotrophs. One possibility is that the IBTX- or paxilline-induced depolarization of the baseline potential shifts the pattern of AP firing from plateau bursting to single spiking. In thalamocortical neurons, for example, sustained membrane depolarization by current injection and the ensuing inactivation of T-type VGCC shifts the pattern of AP firing from bursting to single spiking (McCormick and Pape, 1990). To test whether depolarization of the baseline potential itself is sufficient to shift the pattern of AP firing in spontaneously active somatotrophs, we depolarized the membrane potential in a nonreceptor- and receptor-mediated manner, using KCl and GHRH, respectively. In five separate somatotrophs the addition of 5 mM KCl (total KCl concentration, 9.7 mM) depolarized the baseline potential and increased the burst frequency from 0.19 ± 0.06 to 0.29 ± 0.05 Hz ($p < 0.05$) but did not change the profile of the AP waveform (Fig. 4A,B). Similarly, membrane depolarization by 100 nM GHRH increased the frequency of bursting from 0.16 ± 0.03 to 0.42 ± 0.08 Hz ($p < 0.05$; $n = 8$) but did not induce tonic spiking (Fig. 4C,D).

In addition to shifting the pattern of AP firing from plateau bursting to single spiking, the application of BK channel blockers increased the peak spike amplitude (Figs. 3C,D, 5A, Table 1), indicating that BK channel activation truncates spike amplitude in rat somatotrophs. In general, the spike amplitude determines the magnitude of delayed rectifying (DR) channel activation, which in turn controls the rate and magnitude of membrane repolarization and thus the capacity of AP firing to drive Ca^{2+} entry (Van Goor et al., 2000). To test whether BK channels limit DR channel activation, we determined the peak I_{DR} evoked by different peak spike amplitudes from the current–voltage relation of the isolated I_{DR} (for details, see Materials and Methods). In response to 1 sec depolarizing steps from -80 to $+20$ mV (holding potential, -90 mV), a slowly activating and inactivating I_{DR} was observed (Fig. 5B). The I_{DR} measured at early (0–25 msec) times activated at membrane potentials more depolarized than -30 mV (Fig. 5C, filled circles), whereas the I_{DR} measured at late (990–1000 msec) times was observed at membrane potentials more depolarized than -40 mV (Fig. 5C, open circles). The discrepancy in the apparent activation potentials of the early and late I_{DR} was attributable to the relatively slow activation of this current in somatotrophs (Fig. 5D). Within the range of peak spike amplitudes reached during plateau bursting and paxilline- or IBTX-induced single spiking (-10 to $+10$ mV), there was a marked increase in the peak I_{DR} (≈ 14 pA/mV), as illustrated in Figure 5, A and C.

We next examined whether the membrane potential remained depolarized for a sufficient period of time during the relatively rapid single spike to activate significantly more I_{DR} than during plateau-bursting activity. To do this, we monitored the magnitude and kinetics of I_{DR} activation in response to the application of a single spike or plateau burst in somatotrophs by the AP clamp recording technique. Prerecorded APs from a spontaneously active gonadotroph (spike AP) and somatotroph (burst AP) were used as the command potential waveforms in the voltage-clamp recording mode (Fig. 6A). Under isolated I_{DR} recording conditions (for details, see Materials and Methods) both AP waveforms activated I_{DR} in somatotrophs. However, the peak I_{DR} amplitude evoked by the spike AP was much higher than that evoked by the burst AP (Fig. 6B). In response to the spike AP, the I_{DR} activated during the spike upstroke, reached peak amplitude during the repolarization phase, and returned to baseline levels during the interspike membrane potential (Fig. 6C, left panel). In response to the burst AP, the I_{DR} also activated during the upstroke of the initial spike and reached peak amplitude during the repolarization phase. After the initial spike, however, the I_{DR} did not return to the baseline levels that were observed before the AP waveform (Fig. 6C, right panel), resulting in sustained activation of I_{DR} during the plateau potential. These results indicate that, despite the slow activation of I_{DR} (Fig. 5D), the membrane potential during single spiking remained depolarized for a sufficient period
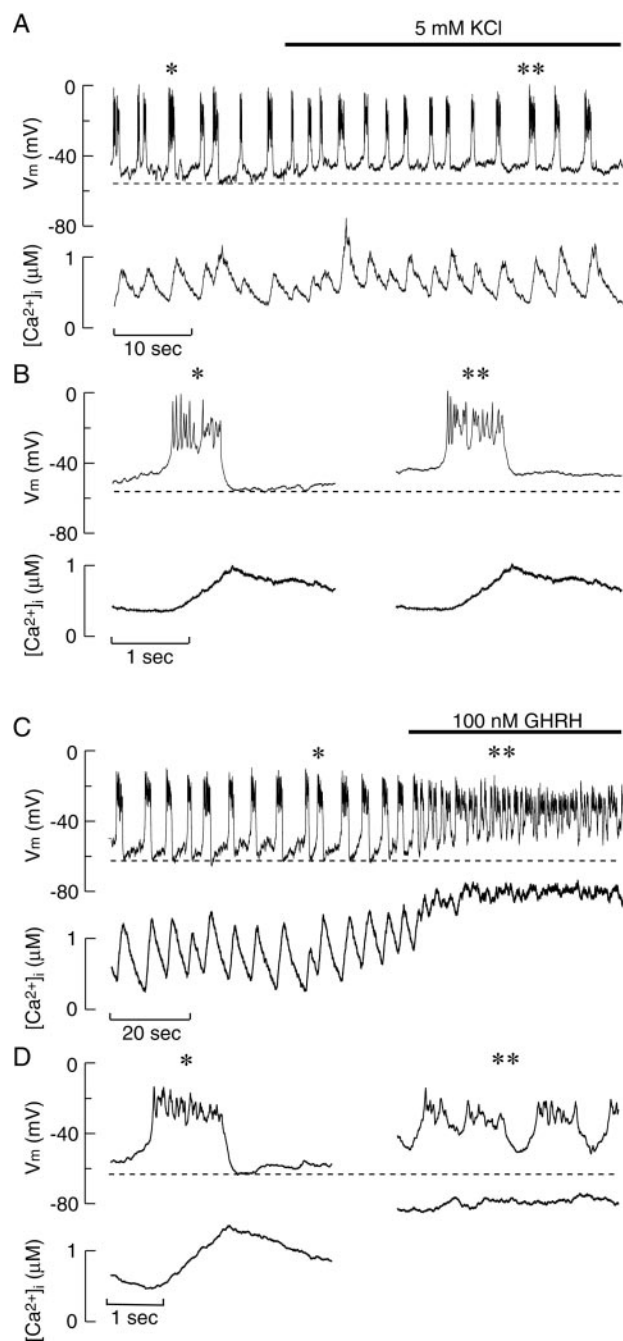
Figure 4. Effects of KCl- and GHRH-induced membrane depolarization on the pattern of AP firing in somatotrophs. *A*, Simultaneous measurement of membrane potential and $[Ca^{2+}]_i$ before and during the application of 5 mM KCl (*horizontal bar*) in a spontaneously active somatotroph. *B*, Expanded time scale of the AP and associated $[Ca^{2+}]_i$ signals before (*single asterisks*) and during (*double asterisks*) KCl application. *C*, Simultaneous measurement of membrane potential and $[Ca^{2+}]_i$ before and during the application of 100 nM GHRH (*horizontal bar*) in a spontaneously active somatotroph. *D*, Expanded time scale of the AP and associated $[Ca^{2+}]_i$ signals before (*single asterisks*) and during (*double asterisks*) KCl application. *Dashed lines* indicate the baseline potential before the application of KCl or GHRH.

of time to activate significantly more I_{DR} than that evoked by the lower amplitude spikes during plateau-bursting activity.

On the basis of these results, an increase in spike amplitude caused by the inhibition of BK channels should activate signifi-

cantly more I_{DR}, which would facilitate spike repolarization and reduce AP-driven Ca^{2+} entry. To test this, we estimated the total current contributing to spike repolarization before and during BK channel inhibition by IBTX by multiplying the rate of spike repolarization (dV_m/dt) by the membrane capacitance (C_m; 4.6 ± 0.2 pF). During plateau bursting the repolarization rate of the initial spike was 2.3 ± 0.2 mV/msec, which corresponds to a net current of 10.6 ± 1.1 pA. Application of 100 nM IBTX significantly ($p < 0.01$; $n = 14$) increased the spike repolarization rate to 3.9 ± 0.3 mV/msec and the net current to 17.9 ± 1.3 pA. Therefore, despite BK channel inhibition there was more net outward current contributing to spike repolarization during single spiking than during plateau bursting. Moreover, these results indicate that BK channel activation truncates the peak spike amplitude, which limits the magnitude of DR channel activation.

Rapid activation of BK channels by domain $[Ca^{2+}]_i$

So that the peak spike amplitude can be truncated, which leads to the reduction in I_{DR}, BK channel activation must be rapid. To test this, we simultaneously monitored I_{BK} and bulk $[Ca^{2+}]_i$ in response to a modified two-pulse protocol. This protocol consisted of a series of Ca^{2+} influx steps ranging in duration from 0 to 300 msec, each of which was followed by a 1 sec test pulse to +90 mV (holding potential, −90 mV). In addition, to monitor the slow decline in bulk $[Ca^{2+}]_i$, we held the membrane potential at −90 mV for 10 sec after the termination of the test pulse (Fig. 7*A*). In response to incremental increases in the duration of the Ca^{2+} influx step, there was a progressive increase in both the peak I_{BK} (Fig. 7*B,D*) and bulk $[Ca^{2+}]_i$ (Fig. 7*C,D*).

However, the expanded time scale of the current and $[Ca^{2+}]_i$ tracings indicated that there was a dissociation in the kinetics of the I_{BK} and bulk $[Ca^{2+}]_i$ profiles (Fig. 7*E–H*). Specifically, brief Ca^{2+} influx steps (<20 msec) did not change the bulk $[Ca^{2+}]_i$ but activated the I_{BK}. In addition, I_{BK} decreased rapidly when Ca^{2+} influx was terminated by stepping the membrane potential to +90 mV (Fig. 7*F*). Although there was a progressive increase in both I_{BK} and bulk $[Ca^{2+}]_i$ in response to longer (≥ 25 msec) Ca^{2+} influx steps, I_{BK} decreased during the slow rise in bulk $[Ca^{2+}]_i$ (Fig. 7*G,H*). Because of the rapid association kinetics of Ca^{2+} binding to indo-1 ($k_{on} = 5 \times 10^8$ M/sec; Jackson et al., 1987), it is unlikely that the slow rise in the reported $[Ca^{2+}]_i$ is attributable to the inability of the Ca^{2+} indicator dye to follow the rise in bulk $[Ca^{2+}]_i$. Moreover, because of the discrepancy in the kinetics of the bulk $[Ca^{2+}]_i$ and I_{BK}, these results suggest that at least a fraction of the BK channels in somatotrophs responds to the rapid, high-amplitude increase in submembrane $[Ca^{2+}]_i$ in the vicinity of the VGCC (heretofore referred to as the domain $[Ca^{2+}]_i$).

To test whether the rapid activation of BK channels is attributable to their activation by domain $[Ca^{2+}]_i$, we used two different calcium buffers, BAPTA and EGTA, which bind Ca^{2+} with a similar affinity but at different rates. Because BAPTA ($k_{on} = 6 \times 10^8$ M/sec; Tsien, 1980) binds Ca^{2+} ~100× faster than EGTA ($k_{on} = 1.5 \times 10^6$ M/sec; Tsien, 1980; Adler et al., 1991), it should be more effective at buffering domain $[Ca^{2+}]_i$. Consequently, it should also be more effective than EGTA at inhibiting BK channels that respond to fluctuations in domain $[Ca^{2+}]_i$. A similar approach has been used to investigate the relationship between BK channel activity and domain $[Ca^{2+}]_i$ in other cell types (Roberts, 1993; Robitaille et al., 1993).

The exogenous Ca^{2+} buffers were introduced into the cytoplasm via the recording electrode by standard whole-cell record-
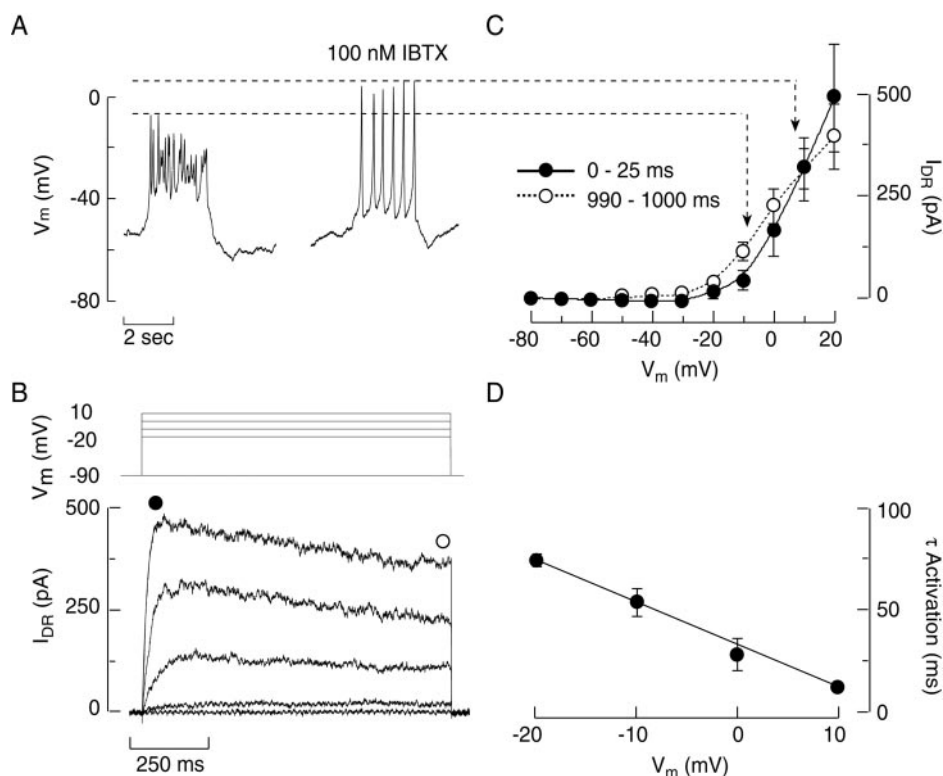
Figure 5. Relationship between spike amplitude and delayed rectifying K^+ channel activation in somatotrophs. *A,* Simultaneous measurement of membrane potential and $[Ca^{2+}]_i$ before and during the application of 100 nM IBTX in a spontaneously active somatotroph. The *dashed lines* indicate the change in peak spike amplitude with and without (*IBTX*) BK channel activation. *B,* Representative tracing of the isolated delayed rectifying K^+ current (I_{DR}) in response to 1 sec membrane potential steps from a holding potential of -90 mV to -90, -20, -10, 0, and 10 mV. *C,* Current–voltage relation of the early (0–25 msec; *filled circles*) and late (990–1000 msec; *open circles*) I_{DR} evoked by 1 sec membrane potential steps from -80 to 20 mV (holding potential, -90 mV; mean $\pm$ SEM; $n = 6$). *D,* Time constant (τ) of I_{DR} activation during 1 sec membrane potential steps from a holding potential of -90 mV to -20, -10, 0, and 10 mV. The time constant of activation for the I_{DR} was best determined by a single exponential fit.
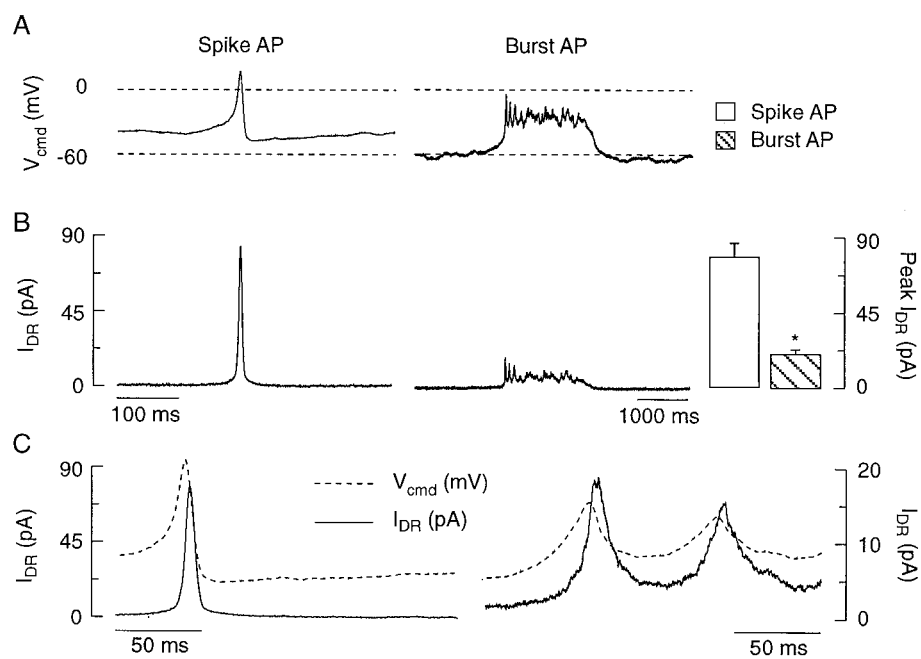

Figure 6. Delayed rectifying I_K evoked by prerecorded single spike and plateau-burst command potentials in somatotrophs. *A,* A single spike (*Spike AP*) and plateau-burst (*Burst AP*) AP waveform were prerecorded from a spontaneously active gonadotroph and somatotroph, respectively, and then used as the command potential under voltage-clamp recording conditions. *B,* Representative current trace of the isolated I_{DR} evoked by the spike (holding potential, -50 mV) and burst (holding potential, -60 mV) AP waveforms in the same somatotroph. The mean $\pm$ SEM of the peak I_{DR} evoked by the spike (*open bar*) and burst (*hatched bar*) AP waveform ($n = 8$) is shown on the *right*. *Asterisks* denote significant differences ($p < 0.01$, paired *t* test). *C,* Expanded time scales of the spike (*left*) and burst (*right*) AP waveforms (*dashed lines*) and the evoked I_{DR} (*solid line*) shown in *A.* Note the different *y*-axis scales between the *left* and *right panels*.

ing techniques, whereas the endogenous Ca^{2+} buffers were preserved with the perforated patch recording technique. In the presence of the endogenous Ca^{2+} buffers of the cell, incremental steps in the duration of Ca^{2+} influx resulted in a progressive increase in the peak I_{BK} amplitude (Fig. 8*A,D*). In the presence of the slow Ca^{2+} buffer, EGTA (100 μM), there was a similar increase in the peak I_{BK} in response to short Ca^{2+} influx steps (<25 msec). However, the peak I_{BK} amplitude evoked by longer Ca^{2+} influx steps (≥ 25 msec) was reduced compared with that in the presence of the endogenous Ca^{2+} buffers (Fig. 8*B,D*). In contrast, the introduction of a similar concentration of the fast

Ca^{2+} buffer, BAPTA (100 μM), into the cytoplasm markedly attenuated I_{BK} activation by both short and prolonged Ca^{2+} influx steps (Fig. 8*C,D*). These results confirm that at least a fraction of the BK channels in somatotrophs is colocalized with VGCCs and responds to the associated fluctuations in domain $[Ca^{2+}]_i$.

Rapid deactivation of BK channels by the clearance of domain $[Ca^{2+}]_i$

In addition to reducing DR channel activation, BK channels also must deactivate and/or inactivate rapidly to prevent full mem-
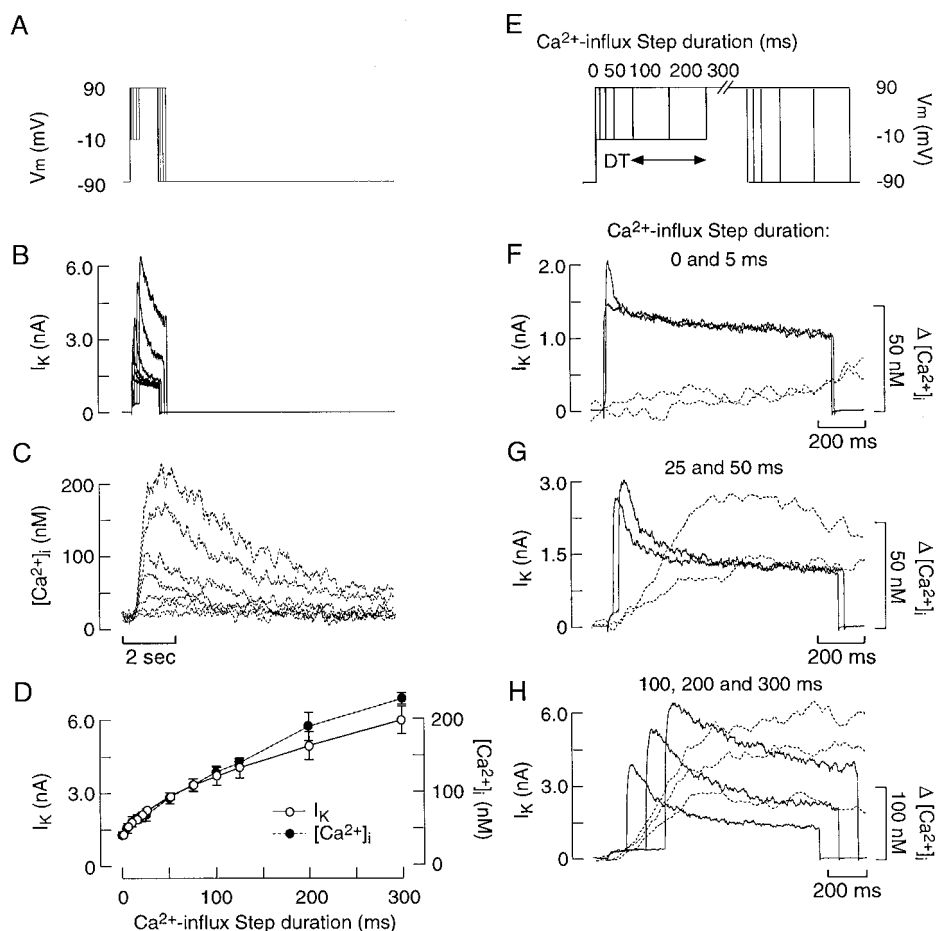
Figure 7. Dissociation between I_{BK} and bulk $[Ca^{2+}]_i$ kinetics in somatotrophs. A series of Ca^{2+} influx steps ranging from 0 to 300 msec was given before the application of a single test pulse to +90 mV (*A*), during which the I_K (*B*) and bulk $[Ca^{2+}]_i$ (*C*) were monitored simultaneously. *D*, The mean ± SEM of the peak I_K (*solid line*) and $[Ca^{2+}]_i$ (*dotted line*) from 19 somatotrophs was plotted against the Ca^{2+} influx step duration. *E*, Expanded time scale of the tracings in *B* and *C* showing both the I_K (*solid lines*) and change in bulk $[Ca^{2+}]_i$ (*dotted lines*) evoked by Ca^{2+} influx steps of 0 and 5 msec (*F*), 25 and 50 msec (*G*), and 100, 200, and 300 msec (*H*) in duration. For clarity, the two-step protocol is not shown to scale, and not all steps are labeled.

brane repolarization and to allow for the generation of the sustained plateau potential. To test this, we first examined the deactivation and/or inactivation kinetics of the I_{BK}. The decrease in I_{BK} during the test pulse may be attributable to deactivation of the BK channels by the rapid clearance of domain $[Ca^{2+}]_i$ and/or voltage-dependent inactivation of these channels (Solaro and Lingle, 1992; Prakriya et al., 1996; Prakriya and Lingle, 2000). To determine whether the BK channels in somatotrophs inactivate, we used a single step protocol, which consisted of 1 sec depolarizing steps from a holding potential of −90 mV to potentials ranging from −80 to +70 mV (Fig. 9*A*). The I_{BK} was isolated by using current subtraction studies as described above. Both the early (0–25 msec; *open circles*) and sustained (990–1000 msec; *filled circles*) I_{BK} activated at membrane potentials more depolarized than −40 mV and were dependent on the underlying I_{Ca}–voltage relation in these cells (Fig. 9*B,C*). The sustained increase in the magnitude of I_{BK} activation during the 1 sec depolarizing steps indicates that the BK channels in somatotrophs do not inactivate. Thus, the rapid decrease in I_{BK} during the relatively gradual rise in bulk $[Ca^{2+}]_i$ (Fig. 7*G,H*) is likely attributable to the deactivation of the channels by the clearance of domain $[Ca^{2+}]_i$ and not to BK channel inactivation.

To demonstrate directly that the decline in I_{BK} is attributable to deactivation, we monitored I_{BK} activation after allowing domain $[Ca^{2+}]_i$ to clear for variable time periods. To do this, we stepped the membrane potential to −10 mV (holding potential, −90 mV) for 5 msec, which was sufficient to activate I_{BK} but did not increase bulk $[Ca^{2+}]_i$ significantly (Fig. 7*F*). Then the mem-

brane potential was stepped back to −90 mV for a variable duration (interstep duration) before being stepped to the test potential of +90 mV, during which I_{BK} was monitored (Fig. 9*D*). In addition to terminating Ca^{2+} influx through VGCCs, the interpulse step to −90 mV also should remove any steady-state inactivation of the BK channels. The magnitude of I_{BK} evoked during the test pulse then was compared with that evoked during the test pulse given immediately after the 5 msec Ca^{2+} influx step. As shown in Figure 9, *E* and *F*, I_{BK} was decreased significantly after only brief interstep durations, confirming that the decline in I_{BK} is attributable to deactivation of the channels by the rapid decrease in domain $[Ca^{2+}]_i$ after the termination of Ca^{2+} influx through VGCCs.

To test whether the rapid deactivation of I_{BK} by the clearance of domain Ca^{2+} prevents BK channels from fully repolarizing the membrane potential, we monitored the amplitude and kinetics of both I_{DR} and I_{BK} activation during plateau-bursting activity via the AP clamp technique (see above). Application of a prerecorded burst AP evoked an outward current, which was reduced by the application of 1 μM paxilline. To isolate the I_{BK} underlying the generation of the burst AP, we subtracted the current evoked in the presence of paxilline from the total current (Fig. 10*A*). Under these conditions I_{BK} was observed during the AP waveform, but not during the interburst period (Fig. 10*A*, *bottom panel*), indicating that BK channels do not contribute to the baseline potential in these cells. We next compared the magnitude and kinetics of I_{DR} and I_{BK} activation during the initial small-amplitude spikes of plateau-bursting activity (Fig. 10*B*).
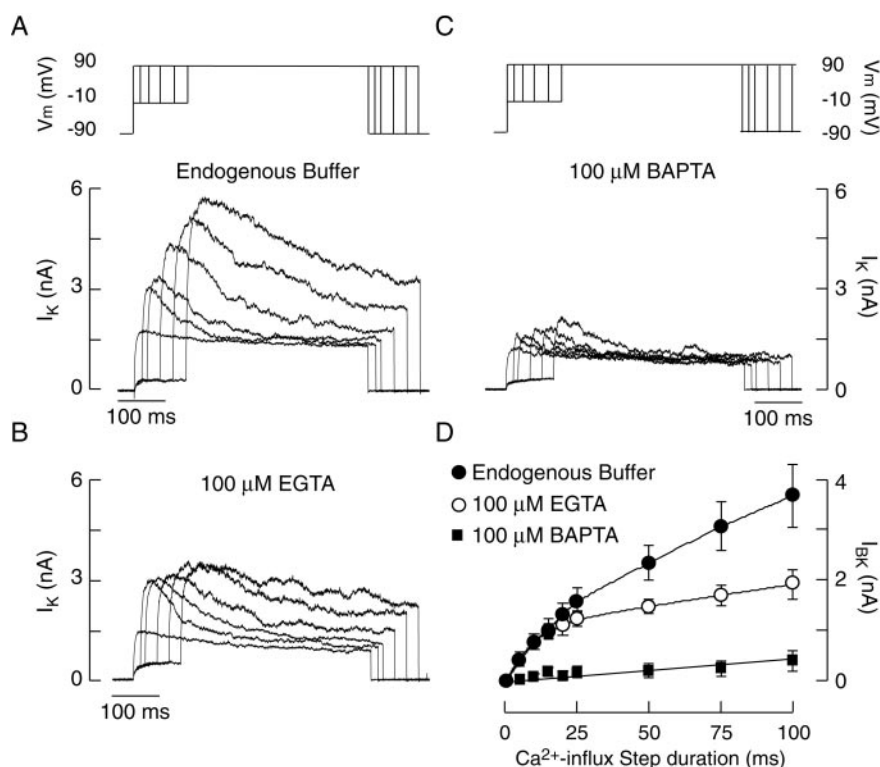
Figure 8. Effects of endogenous and exogenous Ca^{2+} buffers on I_{BK} in somatotrophs. Representative current tracings evoked by the two-pulse protocol in the presence of the endogenous Ca^{2+} buffers (*A*) or the slow and fast exogenous Ca^{2+} buffers, 100 μM EGTA (*B*) and 100 μM BAPTA (*C*), respectively. The endogenous Ca^{2+} buffers were preserved by using the perforated patch recording configuration, whereas the exogenous Ca^{2+} buffers were introduced into the cytoplasm by the recording pipette via standard whole-cell recording techniques. *D*, The mean ± SEM of the isolated I_{BK} evoked by the two-pulse protocol in the presence of the endogenous Ca^{2+} buffers ($n = 15$) or the exogenous Ca^{2+} buffers EGTA ($n = 5$) or BAPTA ($n = 3$).

The I_{BK} rapidly activated during the spike upstroke and then rapidly deactivated during spike repolarization. In contrast, a fraction of the I_{DR} remained activated during the interspike intervals. These results further indicate that I_{BK} rapidly activates during the spike upstroke, which limits spike amplitude and prevents full activation of I_{DR} (Fig. 6*B*). Moreover, I_{BK} also rapidly deactivates during the spike repolarization phase, which prevents full spike repolarization and allows for the generation of the plateau potential and prolonged Ca^{2+} influx.

Addition of BK channels to a gonadotroph model cell converts single spiking to plateau bursting

Our experimental results indicate that the rapid activation/deactivation of BK channels by domain $[Ca^{2+}]_i$ is required for the generation of plateau bursting and the associated high-amplitude $[Ca^{2+}]_i$ transients in somatotrophs. To test this hypothesis further, we examined the impact of increasing BK channel expression in gonadotrophs. Unlike somatotrophs, gonadotrophs express few BK channels and exhibit single-spiking activity that has a low capacity to drive Ca^{2+} entry (Figs. 1, 2). These features were well captured by a mechanistic biophysical model of rat gonadotrophs (Fig. 11*A,B*, *left panels*) previously developed by Li et al. (1995). Spontaneous AP firing in the model is described by a Hodgkin–Huxley-like set of equations, the parameters for which were derived from experimental data obtained from rat gonadotrophs. The major ionic channels contributing AP generation in gonadotrophs include T-type Ca^{2+} channels, L-type Ca^{2+} channels, DR channels, SK channels, and a small leak current (for details, see Materials and Methods).

To simulate the role of BK channels in generating plateau-bursting activity, we introduced these channels into the gonadotroph model cell. On the basis of our experimental results obtained from rat somatotrophs, the kinetics of BK channel activation and deactivation were dependent on the amplitude and kinetics of domain $[Ca^{2+}]_i$ (for details, see Materials and Meth-

ods). Introduction of BK channels into the model shifted the mode of AP firing from single spiking to plateau bursting (Fig. 11*A*, *right panel*), which was similar to that observed in spontaneously active somatotrophs. Specifically, the profile of the AP waveform was characterized by a sustained plateau potential during which multiple small-amplitude single spikes were observed (Fig. 11*B*, *right panel*). In addition, the plateau-bursting activity in the gonadotroph model cell had a higher capacity to drive extracellular Ca^{2+} entry than the single-spiking activity observed in the absence of BK channels. Separation of the underlying currents indicated that rapid BK channel activation by domain $[Ca^{2+}]_i$ truncated the peak spike amplitude (Fig. 11*C*). This reduced the magnitude of DR channel activation, resulting in a decrease in the rate and magnitude of spike repolarization. Moreover, both experimental and mathematical simulations indicate that rapid deactivation of the BK channels by the clearance of domain Ca^{2+} prevents them from fully repolarizing the membrane, allowing for the generation of the plateau potential (Fig. 10*B,C*).

DISCUSSION

In many neuronal, endocrine, and muscle cells, BK channels reduce membrane excitability and the associated Ca^{2+} signals by allowing the passive flux of K^+ from the cell (Kaczorowski et al., 1996; Sah, 1996; Vergara et al., 1998). During AP firing the BK channels are gated by membrane depolarization, and this gating is facilitated by the concomitant increase in Ca^{2+} influx through VGCCs (Stefani et al., 1997). Once open, BK channels act in conjunction with other K^+ channels to facilitate membrane hyperpolarization. This limits the duration of the AP waveform, reducing its capacity to drive extracellular Ca^{2+} entry (Lancaster and Adams, 1986; Lang and Ritchie, 1987; Strom, 1987). BK channel activation also generates the "fast" afterhyperpolarization observed during AP firing in some cell types (Lancaster and

Figure 9. Voltage-dependent inactivation and deactivation properties of I_{BK} in somatotrophs. *A*, To determine whether the BK channels in somatotrophs inactivate during sustained membrane depolarizations, we applied 1 sec depolarizing voltage steps from −90 to +70 mV (holding potential, −90 mV). *B*, Representative current traces of the isolated I_{BK} from nine somatotrophs. The isolated I_{BK} was obtained by subtracting the IBTX- or paxilline-sensitive current from the total current. *C*, Current–voltage relation of the early (*open circles*; 0–25 msec) and late (*filled circles*; 990–1000 msec) I_{BK} shown in *B*. *D*, The relationship between the clearance of domain Ca^{2+} and I_{BK} activation was monitored by using a modified two-pulse protocol, during which the membrane potential was stepped back to −90 mV for 0–300 msec before the application of the test pulse. *E*, Representative current traces evoked by the modified two-pulse protocol. *F*, The mean ± SEM (*n* = 5) of the peak I_K evoked during the test pulse in the absence of a Ca^{2+} influx step and after an interstep interval of 0–300 msec in duration. The *continuous line* is a single exponential fit to the data.
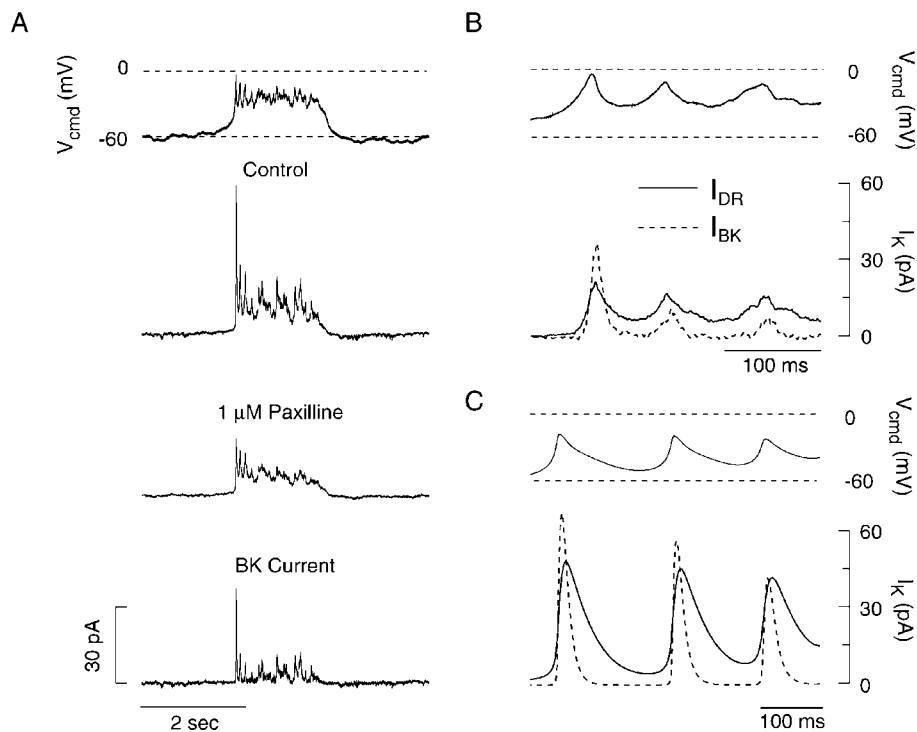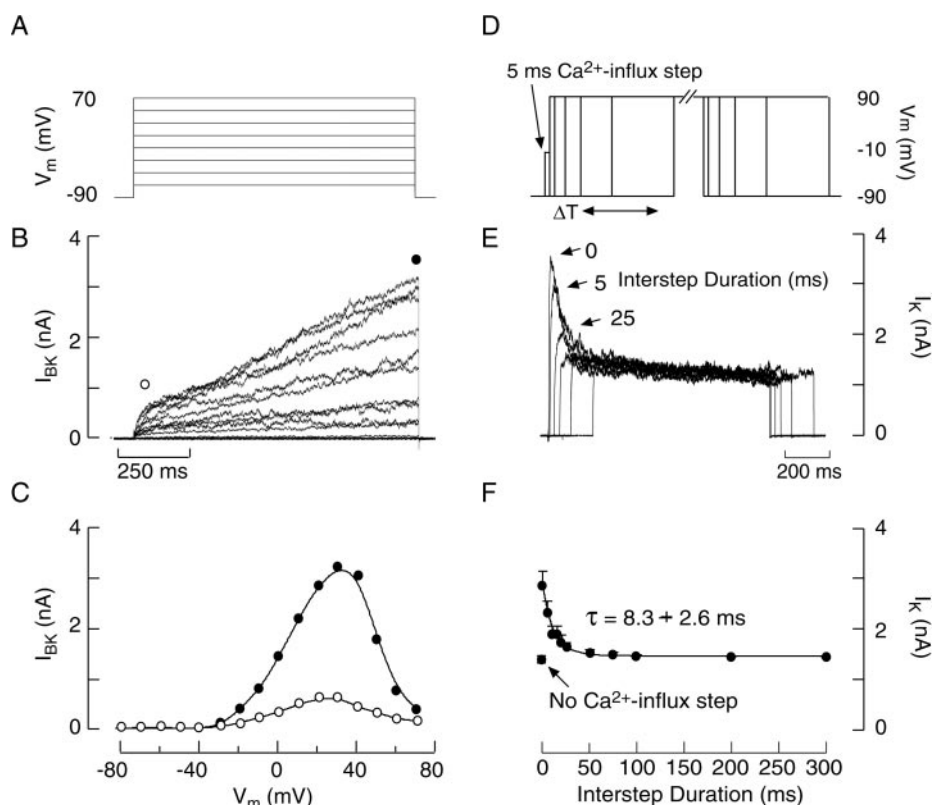

Figure 10. Profile of the I_{DR} and I_{BK} underlying the generation of plateau-bursting activity in somatotrophs. *A*, In seven somatotrophs the I_{BK} evoked by the prerecorded burst AP (*top panel*) was isolated from the I_{DR} by subtracting the paxilline-sensitive current from the total current. Representative current tracings are shown. *B*, Expanded time scale of the burst AP command potential (*top panel*) and the underlying I_{DR} and I_{BK} shown in *A*. *C*, Expanded time scale of the burst AP waveform and the isolated I_{DR} and I_{BK} from the gonadotroph model cell expressing BK channels (Fig. 11*C*, *right panel*, *top* and *bottom traces*).

Adams, 1986). Accordingly, in many different cell types BK channel inhibition by pharmacological blockers (Strom, 1987; Lang and Ritchie, 1989; Pedarzani et al., 2000) or frequency-dependent inactivation (Shao et al., 1999) increases the duration of the AP waveform and the associated Ca^{2+} signals. Thus, by controlling the rate of membrane repolarization and the frequency of firing, BK channels act as a negative feedback pathway to limit AP-driven Ca^{2+} entry.

In rat somatotrophs, however, BK channel activation prolongs AP duration, which facilitates extracellular Ca^{2+} entry. This is supported by four lines of evidence. First, the introduction of rapid Ca^{2+} buffers into the cytosol of somatotrophs prevented BK channel activation and changed the profile of the AP waveform from plateau bursting to single spiking. Second, the inhibition of BK channels by the highly specific BK channel blockers, IBTX or paxilline, also shifted the profile of the AP waveform
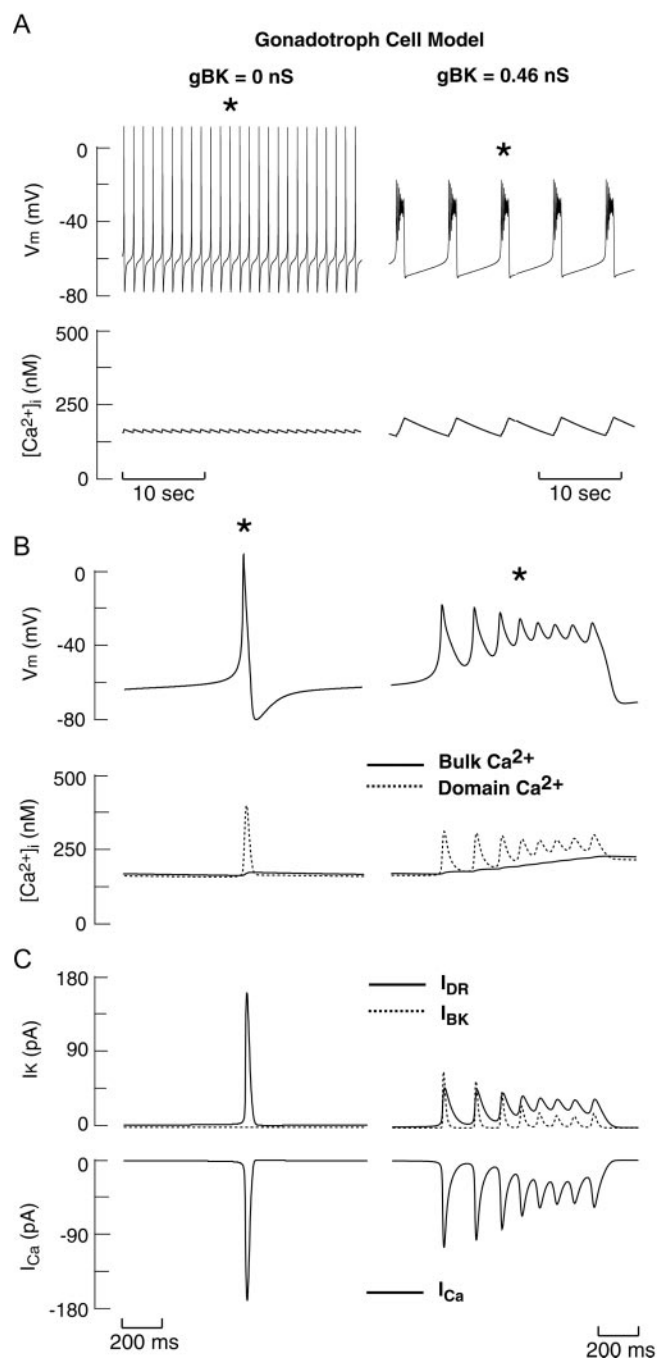
A

Figure 11. Introduction of BK channels into the gonadotroph model cell shifts the pattern of AP firing from single spiking to plateau bursting. *A*, Pattern of AP firing and the associated changes in bulk Ca^{2+} concentration in the gonadotroph model cell in the absence (*left*) and presence (*right*) of BK channels. On the basis of the experimental evidence, BK channels in the model cells responded to fluctuations of domain Ca^{2+} concentration near the opening of the L-type Ca^{2+} channels, whereas SK channels responded to submembrane Ca^{2+} concentrations. *B*, Expanded time scale of the AP and the associated Ca^{2+} transients identified in *A* by the *asterisks*. *C*, Isolated ionic currents underlying the generation of the single spike AP (*left*) and plateau-burst AP (*right*) identified in *B*.

from plateau bursting to single spiking, which reduced its capacity to drive extracellular Ca^{2+} entry. Third, unlike somatotrophs, gonadotrophs express few BK channels and fire single spikes that are not altered by BAPTA, IBTX, or paxilline and have a low capacity to drive Ca^{2+} entry. Finally, the introduction of BK

channels into a mechanistic biophysical model of rat gonadotrophs shifted the pattern of AP firing from single spiking to plateau bursting, which facilitated AP-driven Ca^{2+} entry.

On the basis of our experimental data, we propose the following mechanism for the generation of plateau bursting by BK channels in rat somatotrophs. Activation of VGCCs initiates the AP and generates the first spike. The ensuing Ca^{2+} entry through the VGCC rapidly activates a fraction of the BK channels that are closely associated with the VGCCs. This truncates the spike amplitude well below 0 mV and thereby limits the magnitude of DR channel activation. Together, the BK and DR channels partially repolarize the membrane, leading to the rapid deactivation of BK channels caused by the reduction in Ca^{2+} influx through VGCCs. This leads to a reduction in I_{BK}, and, because the magnitude of DR channel activation is insufficient to repolarize the membrane fully, a plateau potential is generated. The plateau potential is attributable to the balance between the outward I_{DR} and I_{BK} and the inward current through VGCCs. The generation of the plateau potential results in the sustained influx of extracellular Ca^{2+} through VGCCs, resulting in the high-amplitude $[Ca^{2+}]_i$ transients in somatotrophs. The eventual repolarization of the plateau potential may be attributable to the recruitment of additional BK channels and/or activation of SK channels or Ca^{2+}-activated Cl^- channels, both of which have been identified in pituitary cells (Ritchie, 1987; Korn et al., 1991), by the slower and lower amplitude rise in bulk $[Ca^{2+}]_i$. Alternatively, Ca^{2+}-dependent inhibition of VGCCs or the putative cyclic nucleotide-gated channels observed in rat somatotrophs (Tomic et al., 1999) may repolarize the plateau potential.

Critical to the generation of plateau bursting by BK channels is that they activate rapidly enough to truncate the peak spike amplitude, which in turn leads to a reduction in the magnitude of DR channel activation. In addition to responding to domain $[Ca^{2+}]_i$, this indicates that the intrinsic voltage-dependent gating of the BK channels in somatotrophs also must be rapid. Consistent with this, in the absence of accessory β-subunits, which can slow channel activation (Dworetzky et al., 1996), the pore-forming α-subunit of the BK channel has been demonstrated to activate rapidly (<3 msec; Safronov and Vogel, 1998; Araque and Buno, 1999). In addition, in spinal neurons from *Xenopus* embryos the peak magnitude of I_{BK} lagged behind the voltage-gated Ca^{2+} current by <50 μsec (Yazejian et al., 2000), indicating that BK channels can respond rapidly to domain $[Ca^{2+}]_i$. Although the $BK\beta_2$- and $BK\beta_3$-subunits have been identified in the pituitary (Behrens et al., 2000), functional analysis indicates that the $BK\alpha$-subunit is not coupled to any of the known $BK\beta$-subunits *in vivo* (Shipston et al., 1999). In addition, because association of the $BK\beta_2$- and $BK\beta_3$-subunits with the $BK\alpha$-subunit is known to cause inactivation (Uebele et al., 2000; Xia et al., 2000), the lack of BK channel inactivation in rat somatotrophs further indicates that the α-subunit in these cells is not regulated by these β-subunits. It is, therefore, interesting to note that slowing BK channel activation by the association with $BK\beta$-subunits, insertion into the membrane further from the VGCCs, or reducing their sensitivity to Ca^{2+} would prevent them from truncating the spike amplitude and reducing DR channel activation. This, in addition to their delayed activation, would allow them to facilitate membrane repolarization and limit AP-driven Ca^{2+} entry.

Our results indicate that rapid activation of BK channels by domain Ca^{2+} truncates spike amplitude. This limits DR channel activation, allowing for the generation of the prolonged plateau potential that characterizes the low-frequency phasic firing in rat

somatotrophs. The ionic mechanisms underlying the generation of the rhythmic membrane depolarizations that generate the repetitive Na^+–K^+-dependent spiking during phasic firing also have been studied in other cell types. In Purkinje neurons (Raman and Bean, 1997) and "chattering" neocortical neurons (Brumberg et al., 2000) high-frequency burst firing (interburst frequency, 10–40 Hz) has been observed. This high-frequency burst firing is characterized by brief (<100 msec) rhythmic membrane depolarizations on which several high-amplitude fast spikes are observed (intraburst frequency, ~300 Hz). The rhythmic depolarizations are attributable to the repetitive firing of fast afterdepolarizations that are generated by the persistent or resurgent activation of a tetrodotoxin-sensitive Na^+ current (Raman and Bean, 1997; Brumberg et al., 2000). A similar mechanism does not appear to operate in rat somatotrophs, because tetrodotoxin application has no effect on AP-driven $[Ca^{2+}]_i$ transients (Tomic et al., 1999) or plateau-bursting activity (F. Van Goor, unpublished observation).

In thalamocortical neurons, interactions between T-type VGCC and hyperpolarization-activated cationic channels generate low-frequency burst firing (interburst frequency between 0.5 and 10 Hz; Jahnsen and Llinás, 1984a,b; McCormick and Pape, 1990). This low-frequency burst firing is characterized by the rebound activation of T-type VGCC, which generates a transient Ca^{2+} spike with a duration of 100–200 msec. Superimposed on the T-type VGCC spikes are several fast Na^+–K^+-dependent spikes. Repolarization of the burst is attributable to the inactivation of the T-type VGCC channels and is followed by a hyperpolarizing overshoot because of a reduction in the depolarizing influence of hyperpolarization-activated cationic channels. In such cells, sustained membrane depolarizations inactivate T-type VGCC, which abolishes the underlying Ca^{2+} spikes and shifts the pattern of AP firing from bursting to single spiking (McCormick and Pape, 1990). In rat somatotrophs the activation of T-type VGCC appears to be important in initiating the first spike during plateau-bursting activity (Tomic et al., 1999; Van Goor, unpublished observations). In addition to acting as a pacemaker current, a noninactivated fraction of these channels may contribute to the plateau potential and participate in voltage-gated Ca^{2+} entry. However, further studies are required to identify the voltage-gated Ca^{2+} channel subtypes and their contribution to plateau bursting in somatotrophs. The role of VGCC inactivation during burst termination also requires further study.

In conclusion, these results indicate that the differential expression of BK channels between somatotrophs and gonadotrophs underlies the differences in the profile of the AP waveforms and the associated $[Ca^{2+}]_i$ signals. In rat somatotrophs, plateau-bursting activity generates high-amplitude $[Ca^{2+}]_i$ signals, whereas the single-spiking activity in gonadotrophs has a low capacity to drive Ca^{2+} entry. These differences in the pattern of AP firing and the associated $[Ca^{2+}]_i$ likely account for the differences in basal growth hormone and luteinizing hormone secretion in the absence of neuroendocrine regulation.

REFERENCES

Adler EM, Augustine GJ, Duffy SN, Charlton MP (1991) Alien intracellular calcium chelators attenuate neurotransmitter release at the squid giant synapse. J Neurosci 11:1496–1507.

Araque A, Buno W (1999) Fast BK-type channel mediates the Ca^{2+}-activated K^+ current in crayfish muscle. J Neurophysiol 82:1655–1661.

Barrett JN, Magleby KL, Pallotta BS (1982) Properties of single calcium-activated potassium channels in cultured rat muscle. J Physiol (Lond) 331:211–230.

Barry PH (1994) JPCalc, a software package for calculating liquid junction potential corrections in patch-clamp, intracellular, epithelial, and bilayer measurements. J Neurosci Methods 51:107–116.

Behrens R, Nolting A, Reimann F, Schwarz M, Waldschutz R, Pongs O (2000) HKCNMB3 and hKCNMB4, cloning and characterization of two members of the large-conductance calcium-activated potassium channel β-subunit family. FEBS Lett 474:99–106.

Brumberg JC, Nowak LG, McCormick DA (2000) Ionic mechanisms underlying repetitive high-frequency burst firing in supragranular cortical neurons. J Neurosci 20:4829–4843.

Dworetzky SI, Boissard CG, Lum-Ragan JT, McKay MC, Post-Munson DJ, Trojnacki JT, Chang CP, Gribkoff VK (1996) Phenotypic alteration of a human BK (hSlo) channel by hSloβ subunit coexpression: changes in blocker sensitivity, activation/relaxation and inactivation kinetics, and protein kinase A modulation. J Neurosci 16:4543–4550.

Galvez A, Gimenez-Gallego G, Reuben JP, Roy-Contancin L, Feigenbaum P, Kaczorowski GJ, Garcia ML (1990) Purification and characterization of a unique, potent, peptidyl probe for the high conductance calcium-activated potassium channel from venom of the scorpion *Buthus tamulus*. J Biol Chem 265:11083–11090.

Giangiacomo KM, Garcia ML, McManus OB (1992) Mechanism of iberiotoxin block of the large-conductance calcium-activated potassium channel from bovine aortic smooth muscle. Biochemistry 31:6719–6727.

Jackson AP, Timmerman MP, Bagshaw CR, Ashley CC (1987) The kinetics of calcium binding to fura-2 and indo-1. FEBS Lett 216:35–39.

Jahnsen J, Llinás R (1984a) Electrophysiological properties of guinea-pig thalamic neurons, an *in vitro* study. J Physiol (Lond) 349:205–226.

Jahnsen J, Llinás R (1984b) Ionic basis for the electroresponsiveness and oscillatory properties of guinea-pig thalamic neurons *in vitro*. J Physiol (Lond) 349:227–246.

Kaczorowski GJ, Knaus HG, Leonard RJ, McManus OB, Garcia ML (1996) High-conductance calcium-activated potassium channels: structure, pharmacology, and function. J Bioenerg Biomembr 28:255–267.

Kao JPY (1994) Practical aspects of measuring $[Ca^{2+}]_i$ with fluorescent indicators. Methods Cell Biol 40:155–181.

Knaus HG, McManus OB, Lee SH, Schmalhofer WA, Garcia-Calvo M, Helms LM, Sanchez M, Giangiacomo K, Reuben JP, Smith AB (1994) Tremorgenic indole alkaloids potently inhibit smooth muscle high-conductance calcium-activated potassium channels. Biochemistry 33:5819–5828.

Korn SJ, Bolden A, Horn R (1991) Control of action potentials and Ca^{2+} influx by the Ca^{2+}-dependent chloride current in mouse pituitary cells. J Physiol (Lond) 439:423–437.

Koshimizu T-A, Tomic M, Wong AO-L, Zivadinovic D, Stojilkovic SS (2000) Characterization of purinergic receptors and receptor-channels expressed in anterior pituitary cells. Endocrinology 141:4091–4099.

Kwiecien R, Hammond C (1998) Differential management of Ca^{2+} oscillations by anterior pituitary cells: a comparative overview. Neuroendocrinology 68:135–151.

Lancaster B, Adams PR (1986) Calcium-dependent current generating the afterhyperpolarization of hippocampal neurons. J Neurophysiol 55:1268–1282.

Lang DG, Ritchie AK (1987) Large and small conductance calcium-activated potassium channels in the GH_3 anterior pituitary cell line. Pflügers Arch 410:614–622.

Lang DG, Ritchie AK (1989) Tetraethylammonium blockade of apamin-sensitive and -insensitive Ca^{2+}-activated K^+ channels in a pituitary cell line. J Physiol (Lond) 425:117–132.

Lewis DL, Goodman MB, Paul A, Barker JL (1988) Calcium and fura-3 signals in fluorescence-activated cell sorted lactotrophs and somatotrophs of rat anterior pituitary. Endocrinology 123:611–621.

Li Y-X, Rinzel J, Vergara L, Stojilkovic SS (1995) Spontaneous electrical and calcium oscillations in pituitary gonadotrophs. Biophys J 69:785–795.

McCormick DA, Pape H-C (1990) Properties of hyperpolarization-activated cation current and its role in rhythmic oscillation in thalamic relay neurons. J Physiol (Lond) 43:291–318.

Muller EE, Locatelli V, Cocchi D (1999) Neuroendocrine control of growth hormone secretion. Physiol Rev 79:511–607.

Neher E (1998) Usefulness and limitations of linear approximations to the understanding of Ca^{2+} signals. Cell Calcium 24:345–357.

Pedarzani P, Kulik A, Muller M, Ballanyi K, Stocker M (2000) Molecular determinants of Ca^{2+}-dependent K^+ channel function in rat dorsal vagal neurons. J Physiol (Lond) 527:283–290.

Prakriya M, Lingle CJ (2000) Activation of BK channels in rat chromaffin cells requires summation of Ca^{2+} influx from multiple Ca^{2+} channels. J Neurophysiol 84:1123–1135.

Prakriya M, Solaro CR, Lingle CJ (1996) $[Ca^{2+}]_i$ elevations detected by BK channels during Ca^{2+} influx and muscarine-mediated release of Ca^{2+} from intracellular stores in rat chromaffin cells. J Neurosci 16:4344–4359.

Rae J, Cooper K, Gates P, Watsky M (1991) Low access resistance perforated patch recordings using amphotericin B. J Neurosci Methods 37:15–26.

Raman IM, Bean BP (1997) Resurgent sodium current and action po-

tential formation in dissociated cerebellar Purkinje neurons. J Neurosci 17:4517–4526.

Ritchie A (1987) Two distinct calcium-activated potassium currents in a rat anterior pituitary cell line. J Physiol (Lond) 385:591–609.

Roberts WM (1993) Spatial calcium buffering in saccular hair cells. Nature 363:74–76.

Robitaille R, Garcia ML, Kaczorowski GJ, Charlton MP (1993) Functional colocalization of calcium and calcium-gated potassium channels in control of transmitter release. Neuron 11:645–655.

Safronov BV, Vogel W (1998) Large conductance Ca^{2+}-activated K^+ channels in the soma of rat motoneurons. J Membr Biol 162:9–15.

Sah P (1996) Ca^{2+}-activated K^+ currents in neurons: types, physiological roles, and modulation. Trends Neurosci 19:150–154.

Sanchez M, McManus OB (1996) Paxilline inhibition of the α-subunit of the high-conductance calcium-activated potassium channel. Neuropharmacology 35:963–968.

Sealfon SC, Weinstein H, Millar RP (1997) Molecular mechanisms of ligand interaction with the gonadotropin-releasing hormone receptor. Endocr Rev 18:180–205.

Shao L-R, Halvorsrud R, Borg-Graham L, Strom JF (1999) The role of BK-type Ca^{2+}-dependent K^+ channels in spike broadening during repetitive firing in rat hippocampal pyramidal cells. J Physiol (Lond) 521:135–146.

Shipston MJ, Duncan RR, Clark AG, Antoni FA, Tian L (1999) Molecular components of large conductance calcium-activated potassium (BK) channels in mouse pituitary corticotropes. Mol Endocrinol 13:1728–1737.

Smith G, Dai L, Miura RM, Sherman A (2001) Asymptotic analysis of buffered calcium diffusion near a point source. SIAM J Appl Math, in press.

Solaro CR, Lingle CJ (1992) Trypsin-sensitive, rapid inactivation of a calcium-activated potassium channel. Science 257:1694–1698.

Stefani E, Ottolia M, Noceti F, Olcese R, Wallner M, Latorre R, Toro L (1997) Voltage-controlled gating in a large conductance Ca^{2+}-sensitive K^+ channel (hslo). Proc Natl Acad Sci USA 94:5427–5431.

Stojilkovic SS, Catt KJ (1992) Calcium oscillations in anterior pituitary cells. Endocr Rev 13:256–280.

Stojilkovic SS, Izumi S-I, Catt KJ (1988) Participation of voltage-sensitive calcium channels in pituitary hormone release. J Biol Chem 263:13054–13061.

Stojilkovic SS, Kukuljan M, Iida T, Rojas E, Catt KJ (1992) Integration of cytoplasmic calcium and membrane potential oscillation maintains calcium signaling in pituitary gonadotrophs. Proc Natl Acad Sci USA 89:4081–4085.

Strom JF (1987) Action potential repolarization and fast afterhyperpolarization in rat hippocampal pyramidal cells. J Physiol (Lond) 385:733–759.

Tomic M, Koshimizu T, Yuan D, Andric SA, Zivadinovic D, Stojilkovic SS (1999) Characterization of a plasma membrane calcium oscillator in rat pituitary somatotrophs. J Biol Chem 274:35693–35702.

Tse A, Hille B (1992) GnRH-induced Ca^{2+} oscillations and rhythmic hyperpolarizations of pituitary gonadotropes. Science 255:462–464.

Tsien RY (1980) New calcium indicators and buffers with high selectivity against magnesium and protons: design, synthesis, and properties of prototype structures. Biochemistry 19:2396–2404.

Uebele VN, Lagrutta A, Wade T, Figueroa DJ, Liu Y, McKenna E, Austin CP, Bennett PB, Swanson R (2000) Cloning and functional expression of two families of β-subunits of the large conductance calcium-activated K^+ channel. J Biol Chem 275:23211–23218.

Van Goor F, Le Beau A, Krsmanovic LZ, Catt KJ, Sherman A, Stojilkovic SS (2000) Amplitude-dependent spike-broadening and enhanced Ca^{2+} signaling in GnRH-secreting neurons. Biophys J 79:1310–1323.

Vergara C, Latorre R, Marrion NV, Adelman JP (1998) Calcium-activated potassium channels. Curr Opin Neurobiol 8:321–329.

Xia X-M, Ding J-P, Zeng X-H, Duan K-L, Lingle CJ (2000) Rectification and rapid activation at low Ca^{2+} of Ca^{2+}-activated, voltage-dependent BK currents: consequences of rapid inactivation by a novel β-subunit. J Neurosci 20:4890–4903.

Yazejian B, Sun X-P, Grinnell AD (2000) Tracking presynaptic Ca^{2+} dynamics during neurotransmitter release with Ca^{2+}-activated K^+ channels. Nat Neurosci 3:566–571.